INVESTIGATION OF THIN FILM MODULATOR FOR 10 MICRON LASERS

P. K. Cheo

United Aircraft Research Laboratories

Prepared for:

Advanced Research Projects Agency
Office of Naval Research

30 March 1973

THIN FILM MODULATOR FOR 10 micron LASERS

INTERIM TECHNICAL REPORT

PERIOD COVERED : 25 AUGUST 1972 TO 25 MARCH 1973

CONTRACT NO. N00014-73-C-0087

Sponsored by

ADVANCED RESEARCH PROJECTS AGENCY
ARPA ORDER NO. 1806, AMENDMENT NO. 6

United Aircraft
Research Laboratories

UNITED AIRCRAFT CORPORATION

EAST HARTFORD, CONNECTICUT 06108

AD. 757792

M921513-2

Interim Technical Report

Investigation of Thin Film Modulator for 10 Micron Lasers

by

P. K. Cheo
United Aircraft Research Laboratories
East Hartford, Connecticut 06108
(203)565-4297

March 30, 1973

Prepared for the Office of Naval Research
Scientific Contracting Officer-Dr. M. White
Contract N00014-73-C-0087-$49,542.00
25 August 1972 to 23 June 1973

sponsored by
Advanced Research Projects Agency
ARPA Order 1806, Amendment No. 6, 7-18-72

I

Investigation of Thin Film Modulator for 10 Micron Laser

TABLE OF CONTENTS

LIST OF ILLUSTRATIONS

Investigation of Thin Film Modulator for 10 Micron Lasers

1.0 TECHNICAL REPORT SUMMARY

1.1 Program Objectives

The objective of this program is to explore various techniques utilizing GaAs epitaxial thin films as the active elements for electrooptic modulation of the 10.6 μm CO_2 laser radiation. The advantages as well as the limiting factors concerning the use of thin films to perform phase and polarization modulation or switching of infrared laser radiation will be investigated. The results of this program shall provide useful information concerning the possible use of GaAs thin films to replace bulk materials for electrooptic modulation of infrared laser radiation. Furthermore, results of this program may provide a guideline to the design of the master oscillator by taking the advantage of thin film modulator to yield the necessary wave envelope and bandwidth required for the high power pulsed CO_2 laser imaging radar system.

1.2 Major Accomplishments

Under the present ARPA/ONR research program (Contract N00014-73-C-0087), pulse amplitude modulation of a 10-μm CO_2 laser beam in a GaAs electrooptic thin film has been demonstrated (Ref. 1) by steering a guided-wave mode in the plane of the thin film. Attempts were also made to investigate (Ref. 2) other modulation schemes by producing polarization modulation and switching of the infrared radiation in thin films. Preliminary results indicate that electrooptic modulation of the infrared radiation is more difficult to accomplish with the latter two schemes. We have also made a design analysis (Ref. 3) of a master oscillator, which consists of a stable CO_2 laser and a GaAs thin film modulator, to produce a sideband at the sum or difference frequencies at the Ku-band. Efficient electrooptic interaction can occur in a GaAs thin film between an optical guided-wave and either a traveling or a synchronous standing microwave signal. By using a frequency modulated microwave field, a chirped optical signal in the sideband can be generated. Within the framework of the present program, experimental data compiled to-date are sufficient to provide a realistic assessment of thin film waveguide devices versus bulk devices. Our results indicate that electrooptic modulation of CO_2 laser by using a thin film device can reduce rf power required to drive the conventional bulk modulator to a level which is within the reach of the present-day electronic components technology. A typical power reduction by a factor of 10^3 can easily be obtained by using thin film devices.

1.3 Method of Approach

1.3.1 Initial Program Plan

The plan of the initial program was to explore the use of GaAs epitaxial thin films for electrooptic modulator devices that can provide various modulation formats suitable for and compatible with the operation of an optical waveguide. These devices were fabricated by utilizing existing material technology and available GaAs epitaxial thin films.

1.3.2 Revised Program Plan

Based on experimental data compiled to-date, we believe that the replacement of active bulk devices for the modulation of 10-μm CO_2 lasers with thin films is a practical approach. This research program is now being redirected toward the demonstration of efficient generation of a train of chirped CO_2 laser pulses by means of a nonlinear interaction between a traveling microwave and a 10.6 μm guided-wave mode in a GaAs epitaxial thin film waveguide.

1.4 Future Research Plan

For the remaining portion of the present program, efforts will be continued to investigate phase modulation of a guided wave mode in GaAs thin films by means of a super-heterodyne technique as described in Section 2. Additional efforts will be made to investigate other optical coupling techniques including the use of laser interferometric techniques as described in Section 3. Work on material growth and special handling techniques of epi-layers (Ref. 3), which will satisfy both the optical and microwave coupling requirements, will be initiated. Also some preliminary work involving the design and fabrication of a microwave cavity will also be made. This device will provide a test bed for the evaluation of microwave coupling techniques as described in Section 3.

2.0 IR THIN FILM MODULATOR-PRESENT STATUS

2.1 IR Thin Film Waveguide Structure

GaAs epitaxial thin film structures suitable for use as passive and active waveguide devices at the 10-micron CO_2 laser wavelength consists of a low free electron concentration ($N \lesssim 10^{13}$ cm^{-3}) single crystal thin film deposited onto an N type GaAs Bridgman substrate with a N value $\simeq 10^{18}$ cm^{-3}. The use of doping profile to establish the index difference Δn between the epitaxial layer and the substrate is a good choice for lasers at longer wavelength. Because of the large difference in free carrier concentrations the refractive index of N^+ GaAs substrate is depressed significantly below that of the undoped epitaxial layer by an amount given by

$$\Delta n = \frac{e^2 \Delta N}{8n\pi^2 m \epsilon_o c^2} \lambda^2 \qquad (1)$$

where ΔN is the difference in free carrier concentrations, n the refractive index of the layer, m and e are the carrier mass and charge, c is the velocity of light and ϵ the permittivity of free space. For $\lambda = 10.6$ μm, the index difference between an undoped layer and a heavily doped substrate ($N_s = 1.6 \times 10^{18}$ cm^{-3}) can be as large as 0.3. With such a large index difference, a number of discrete modes can be excited and confined in a relatively thin film having a thickness of the order of one optical wavelength.

Consider a waveguide structure as shown in Fig. 1, which consists of a thin film of thickness t with refractive index $n_1 = 3.275$ at 10.6 μm and a substrate with $n_o = 2.975$ ($N_o = 1.6 \times 10^{18}$ cm^{-3}). The medium above this film is air with $n_2 = 1$. Let β_m represent the propagation constant of the mth mode. We have calculated the β_m/k value, where k is the propagation constant in free space, by using the analysis of Tien and Ulrich (Ref. 5). Figure 2 is the plot of a waveguide thickness versus β/k values for the TE and TM modes. The dotted and the solid curves represent the TE and the TM modes, respectively. For lower order modes, the difference between TE and TM is small (degenerate cases). As $m > 2$, differences between TE and TM become more distinguishable. Data shown in Fig. 2 provide the basic information needed for the design of various waveguide devices.

Figure 3(a) is a photograph of one of the large GaAs epitaxial layers. The long axis (110) of this thin film element has a length greater than 1.3 inches. In order to establish carrier concentration levels in the epitaxial layer, both Schottky barrier measurements using a Copeland-type (Ref. 4) profiler to obtain the carrier concentration versus distance X from the surface of the layer, and to a lesser degree, Hall measurements were performed. The essential idea of the Copeland technique is that if a constant AC current ($\omega/2\pi = 5$ MHz) is applied to the reverse-biased metal-semiconductor structure, the voltage at ω is proportional to X while

FIG. 1

CRYSTAL ORIENTATIONS FOR GaAs EPITAXIAL THIN–FILMS

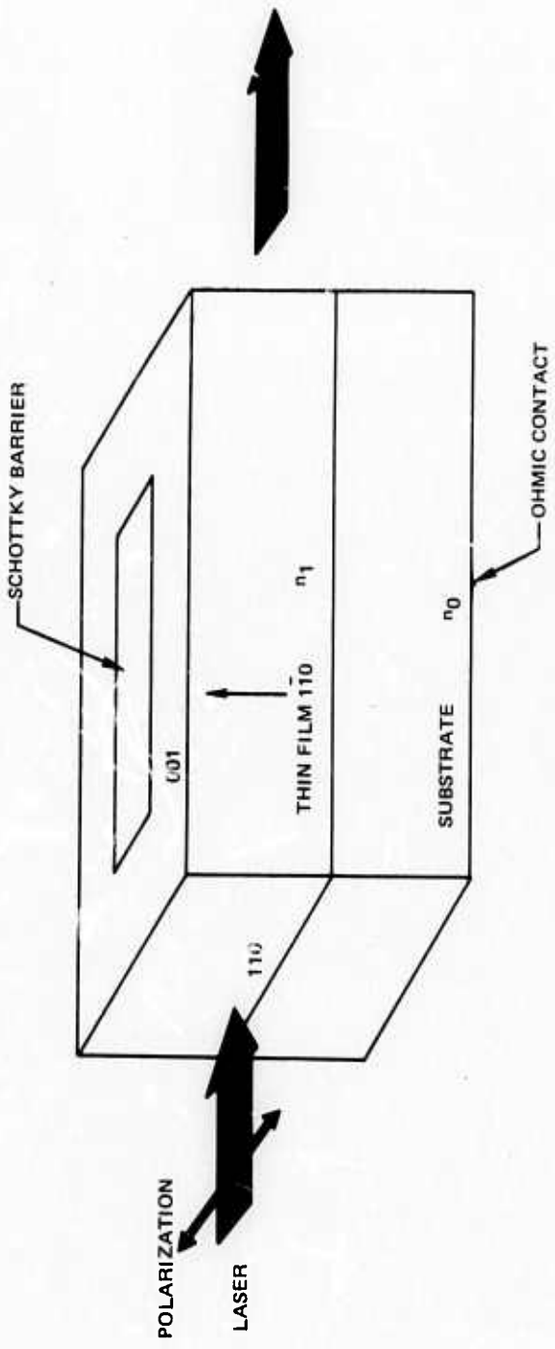

FIG. 2

GaAs FILM THICKNESS VS β/k FOR THE TE AND TM MODES

($n_0 = 2.975$, $n_1 = 3.275$, $n_2 = 1.0$, AND $\lambda = 10.59\ \mu m$)

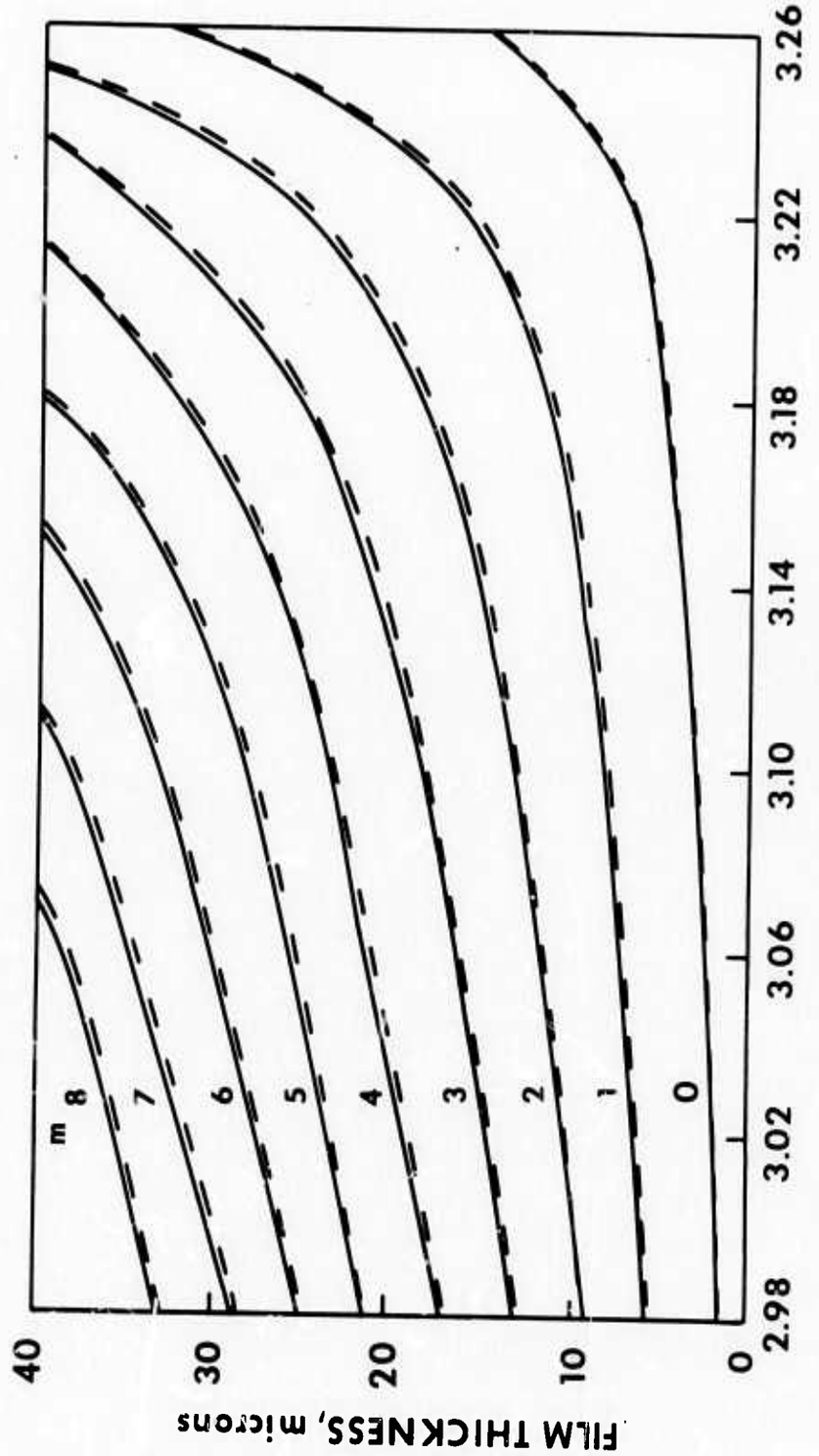

SCHOTTKY BARRIER ELECTRODES AND V–I CHARACTERISTICS OF GaAs THIN FILM (1–51–2A)

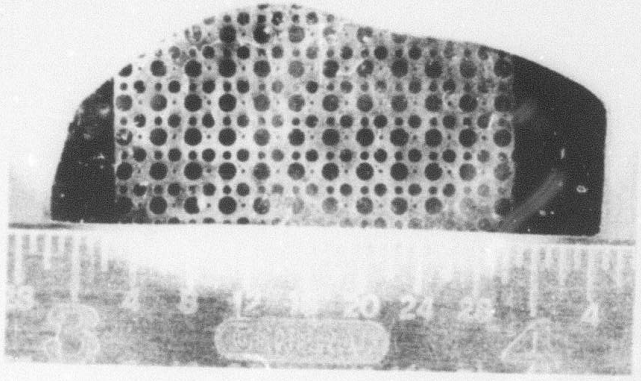

(a)

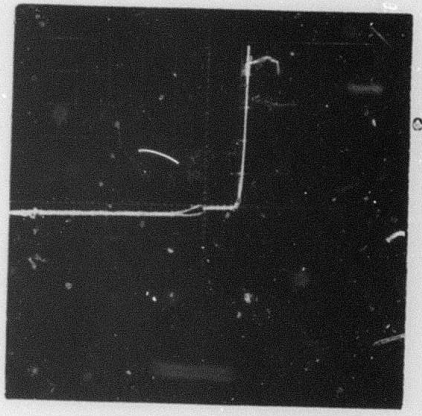

(b)

FIG. 3

a generated voltage at 2ω is inversely proportional to the carrier concentration. Through independent monitoring of the AC voltages and plotting these with respect to each other, a carrier concentration profile results as the DC bias level is changed. Correction for edge-effect errors can be made following profiling (Ref. 5). To prepare the Schottky barrier structures, Au-12% Ge was evaporated onto the lapped substrate side and alloyed to establish ohmic contact. Gold evaporated onto the epitaxial layer and then subjected to standard photolithographic etching to define areas of metallization form the Schottky barrier. Hall measurements were made on epitaxial layers deposited on semi-insulating Cr-doped Bridgman substrates (resistivity > 10^8 ohm-cm). Photolithographic etching defined the Hall mesa, and contacts were made with alloyed Au-12% Ge evaporated onto the arms of the mesa.

The electron concentration in heavily doped substrates (5×10^{17} cm$^{-3} \leq N_o \leq 10^{19}$ cm^{-3}) was obtained by recording the IR wavelength of minimum reflectivity near plasma resonance (Ref. 6). Also, the thickness of the epitaxial layer grown on these substrates was obtained using infrared interferometry via analysis of the fringe separations on the reflectivity-wavelength plot. The electron concentration in material for which $N_o < 5 \times 10^{17}$ cm^{-3} was assigned on the basis of Hall measurements on ultrasonically cut Hall bars taken from nearby slices of the Bridgman boule.

Figure 3(b) shows the typical I-V characteristics of the Schottky barrier electrodes. The reverse breakdown voltage, in this case, is over 100 volts and is a characteristic of the epi-layer surface quality and low free carrier concentration. Figure 4 shows a typical doping profile of the epi-layer (1-51-2A). These results were obtained by Schottky barrier measurements for a number of points along the length of the layer. Noted that the thickness uniformity of this layer is reasonably good to within ± 1 μm over a length of 2.5 cm. The free carrier concentration in this epitaxial layer is < 10^{14} cm^{-3}. Our vapor phase epitaxial system (1EP) has been producing small epitaxial layers (1.5 cm in length) having a free carrier concentration less than 10^{12} cm^{-3}. In these cases the built-in voltage of the Schottky barrier (with no applied DC bias) is sufficient to fully sweep the layer of mobile charge. For example, in the case of a 35-μm layer, the region beneath the Schottky contact will be fully depleted if N is uniformly 10^{12} cm^{-3}. In such a case no profile results except for a thin region at the epi-substrate interface; therefore, the actual carrier concentration in this layer can be surmised. Another important aspect of high resistivity and low N GaAs epitaxial thin film is that for a fixed electrode area and a bias voltage, the capacitance decreases almost exponentially with decreasing N of the epi-layer. Figure 5 is a plot of the capacitance of GaAs epitaxial thin film having a constant Schottky barrier area (0.05 cm^2) as a function of reverse bias voltage. For N = 12 cm^{-3}, the capacitance of a 1 mm x 3 cm GaAs epitaxial thin film would be 18 pF at a reverse bias voltage of 20 volts, and ~ 10 pF at 50 volts.

FIG. 4

DOPING PROFILE OF GaAs EPITAXIAL THIN FILM

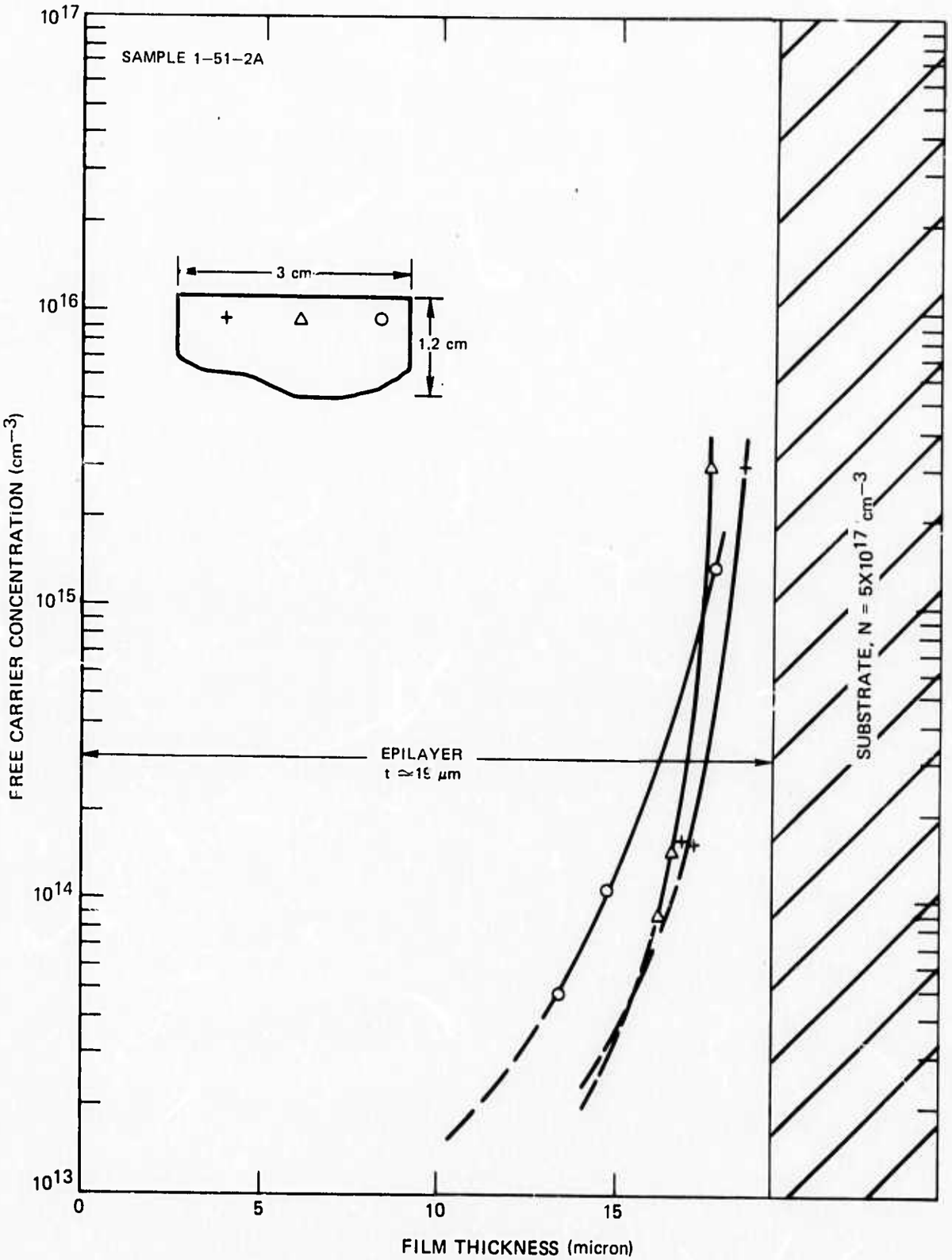

FIG. 5

CAPACITANCE VS BIAS FOR Au–n–GaAs STRUCTURES

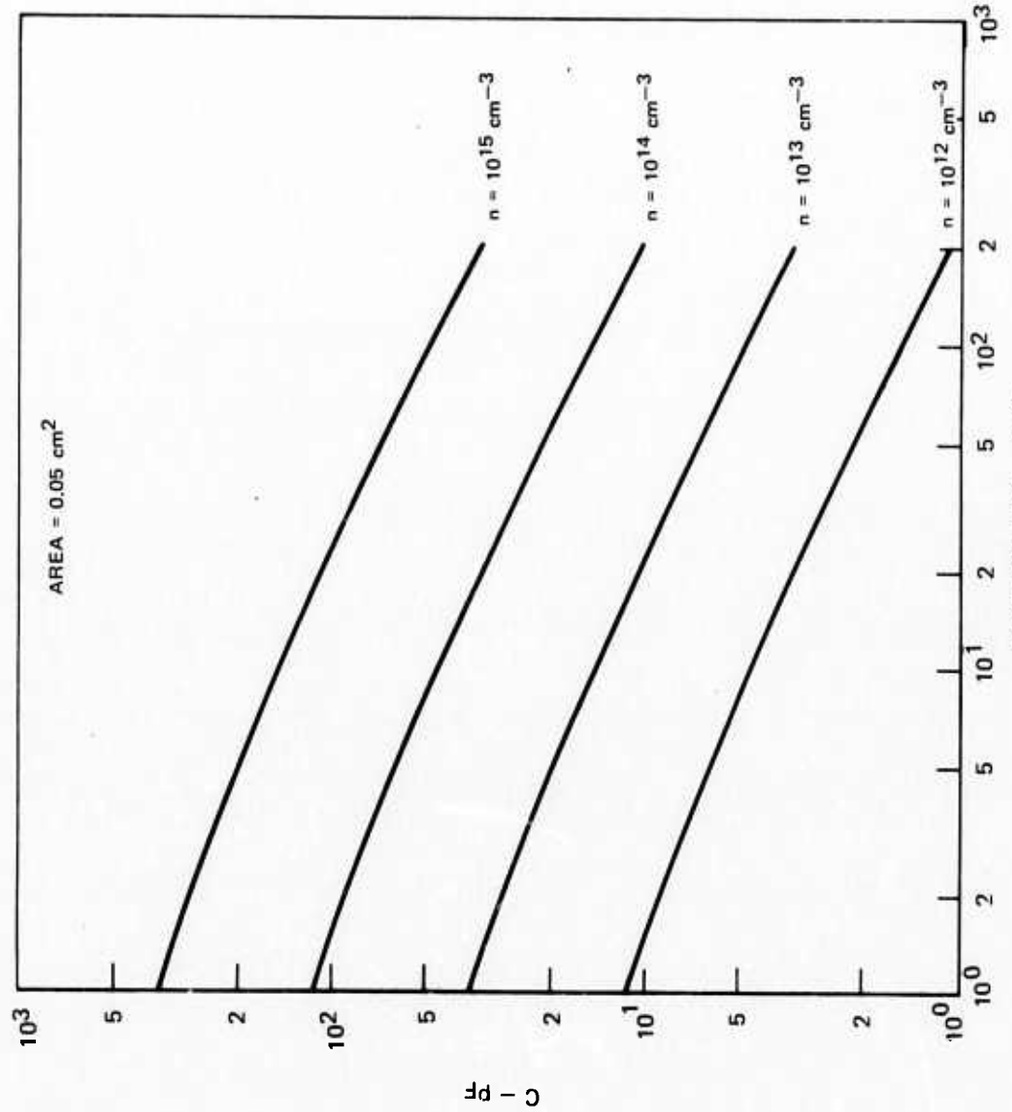

2.2 Electrooptic Modulation

Attempts were made to perform electrooptic modulation of the 10 μm CO_2 laser radiation in GaAs thin films. The 10.6 μm guided-wave modes have been excited by using either Ge prism or etched grating coupler. In the following we shall discuss and present results on three types of electrooptic modulation involving either the amplitude or the phase variation of the 10 μm guided-wave mode in electrooptic GaAs thin films.

2.2.1 Amplitude Modulation

Amplitude modulation can be obtained by varying (1) the ellipticity of light as a result of a phase difference $\Delta\Gamma$ between two orthogonal waves propagating along the waveguide, (2) the waveguide index profile, which has a value very near the cut-off, and (3) the direction of propagation of a guided mode in the thin film. In all cases, a Schottky barrier electrode is deposited on the surface of the epitaxial layer through a SiO_2 mask of the desired pattern, and the N^+ GaAs substrate is alloyed to establish a good ohmic contact. Our calculations (Ref. 2) show that optical attenuation through these thin films in the presence of metallic electrodes is significant, and the loss for TM modes is much more severe than that for the TE modes. Our analyses also show that the loss varies as $1/t^3$, where t is the thickness of the waveguide. To reduce the loss, particularly for polarization modulation, where simultaneous excitation of two orthogonal modes is required, the film thickness must be chosen not less than 30 μm. However, for thicker films the voltage required for electrooptic interaction becomes greater and more difficult it is to excite lower order modes.

Experimentally we have excited a TE and a TM mode simultaneously in a 30 μm thick guide by placing a properly oriented CdS $\lambda/4$ plate in front of the input grating coupler. The radiation coupled out of the output grating coupler was analyzed by a wiregrid polarizer. It was found that the intensity ratio

$$\frac{I_{TM}}{I_{TE}} = \left(\frac{E_{TM}}{E_{TE}}\right)^2 = 0.08 \qquad (2)$$

This measured value is in good agreement with the calculated attenuation rates for the TE and the TM modes. When a voltage V is applied to the Schottky barrier electrode, a phase shift $\Delta\Gamma$ between the TE and TM mode is expected to be

$$\Delta\Gamma = \frac{\pi}{\lambda} n^3 r_{41} \ell \left(\frac{V}{t}\right) \qquad (3)$$

where n is the refractive index, r_{41} is the electrooptic coefficient and ℓ is the length of the electrode. Assuming that the two guided waves at the output grating coupler having the form

$$E_{TM} = A_{TM}\sin\omega t$$
$$E_{TE} = A_{TE}\sin(\omega t-\Delta\Gamma) \tag{4}$$

it is straightforward to show that

$$\left(\frac{E_{TM}}{A_{TE}} - \frac{E_{TM}}{A_{TM}}\right)^2 + \frac{2E_{TE}E_{TM}}{A_{TE}A_{TM}}(1-\cos\Delta\Gamma) - \sin^2\Delta\Gamma = 0 \tag{5}$$

If $\Delta\Gamma = 0$, Eq. (5) reduces to

$$\left(\frac{E_{TE}}{E_{TE}}\right)^2 = \left(\frac{A_{TM}}{A_{TE}}\right)^2 \tag{6}$$

The difference in ellipticity as a result of $\Delta\Gamma$ can be measured by the cross term:

$$\frac{2E_{TE}E_{TM}}{A_{TE}A_{TM}} = \sin^2\Delta\Gamma(1-\cos\Delta\Gamma)^{-1} \tag{7}$$

For V = 50 volts, t = 30 μm and ℓ = 0.5 cm, Eq. (3) gives a $\Delta\Gamma$ value of 0.14 rad (= 8°). For $\Delta\Gamma$ = 8°, we obtain from Eq. (7) that

$$\frac{2E_{TE}E_{TM}}{A_{TE}A_{TM}} \simeq 2 \times 10^{-4} \tag{8}$$

which is a very small difference in ellipticity.

During the course of measuring ellipticity, we observed pulse amplitude modulation of light when a voltage pulse was applied to the Schottky barrier electrode. But it was at first rather surprising to observe a large increase in pulse amplitude when both the analyzer and the λ/4 plate were removed. It turns out that the observed pulse amplitude modulation is caused by beam steering (Ref. 1) of the guided-wave mode propagating along the edge of the Schottky barrier electrode. A switching time of about 60 nsec has been obtained and is limited by the detector response. This technique has been used to obtain more than 12% amplitude modulation of a CO_2 laser by applying only 50 volts to an 20 μm thick GaAs thin film having a total interaction length of 0.5 cm.

Figure 6(a) shows the waveforms of the applied voltage (upper trace) pulse and the modulated light (lower trace) pulse detected by the PbSnTe photodiode located about 10 cm away from the output grating coupler. This light pulse disappears when either the output grating coupler is blocked or the voltage pulse is removed from the Schottky barrier electrode. The voltage pulse, which has a risetime less than 10 nsec, was measured by a FET probe with a 40 dB attenuator at the Schottky barrier electrode. The risetime of the modulated laser pulse is ~ 60 nsec (10% to 90%) a response limited essentially by the response of the IR detector used in our experiment. Figure 6(b) shows a train of short negative-going pulses which appear only when voltage pulses are applied, as shown by the upper trace of Fig. 6(b). The chopped light pulse, L_c, having a pulse width ~ 3.5 msec, represents the unmodulated TE_1 mode intensity transmitted through the waveguide. The intensity of the modulated laser pulses, L_m, was found to increase linearly with increasing V_p and ℓ.

At V_p = 50 volts, we have measured L_m as a function of detector position which was varied by scanning the detector element in the plane of incidence. The aperture of this detector is 0.0018 cm^2. The results, as shown by the dotted curve in Fig. 7 indicate that other modes have also been modulated by the applied E-field in a way similar to that observed for the TE_1 mode. The solid curve represents the unmodulated light transmitted through the waveguide. These results along with the polarization analysis of the modulated laser pulses rule out mode conversion process (Refs. 7,8), i.e., $TE_i \rightarrow TE_j \rightarrow TE_i \rightarrow TM_i$, as a possible mechanism responsible for the decrease of laser power in the presence of electric field. Further investigation reveals that the negative-going pulse does not represent a loss of laser power, in fact, it corresponds to a beam steering of the guided TE_1 mode in the plane of the thin film. By moving the detector element in the direction perpendicular to the plane of incidence, we observed that the amplitude of the modulated laser pulse changes from a negative to a positive value with respect to the chopped laser pulse as shown in Fig. 8. Simultaneous measurements of L_c and L_m as a function of detector displacement along a line perpendicular to the plane of incidence are plotted in Fig. 9. The results show that the modulated beam is shifted away from the electrooptically active region by an angle $\alpha \simeq 1.1$ mrad for V_p = 50 volts, and ℓ = 0.5 cm. It was observed that the pulse amplitude of the modulated light is greatest when the guided-wave mode is propagating along the edge of the Schottky barrier electrode. The electrooptic change in refractive index for light propagating along the (011) direction is

$$\Delta n_{EO} = -\tfrac{1}{2} n^3 r_{41} \frac{V}{t} \qquad (9)$$

where n, r_{41} and t are the refractive index, electrooptic coefficient and the thickness of the guiding film, respectively. The difference in refractive index between the active and nonactive region of the guiding film can cause the observed beam steering effect as a result of reconstruction of the wavefront of two plane waves having a slight phase difference $\Delta\Gamma = k\ell\Delta n_{EO}$, propagating along the edge of the electrode. Based on this model we can qualitatively estimate the angle of deflection α by the expression

FIG. 6

PULSE AMPLITUDE MODULATION OF A CO_2 LASER IN A GaAs THIN FILM

a)

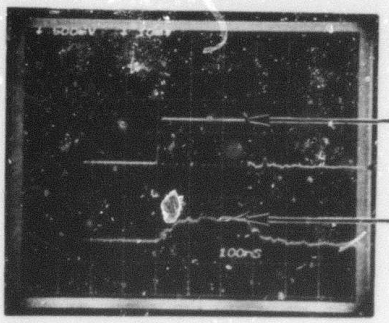

V_p

L_m

b)

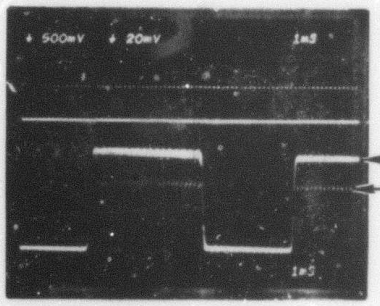

L_c

L_m

FIG. 7

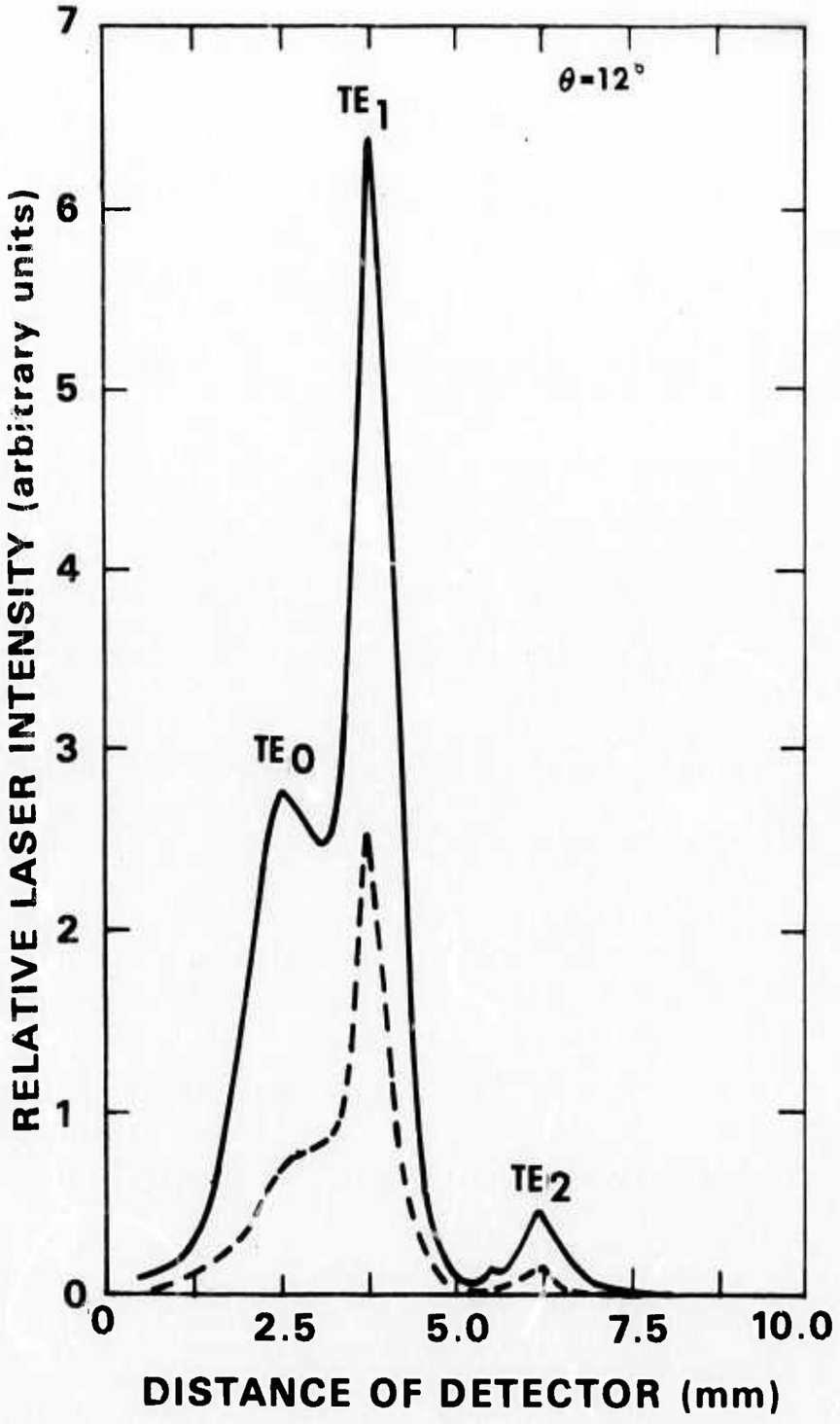
θ=12°
TE1
TE0
TE2
RELATIVE LASER INTENSITY (arbitrary units)
DISTANCE OF DETECTOR (mm)
0
1
2
3
4
5
6
7
0
2.5
5.0
7.5
10.0

FIG. 8

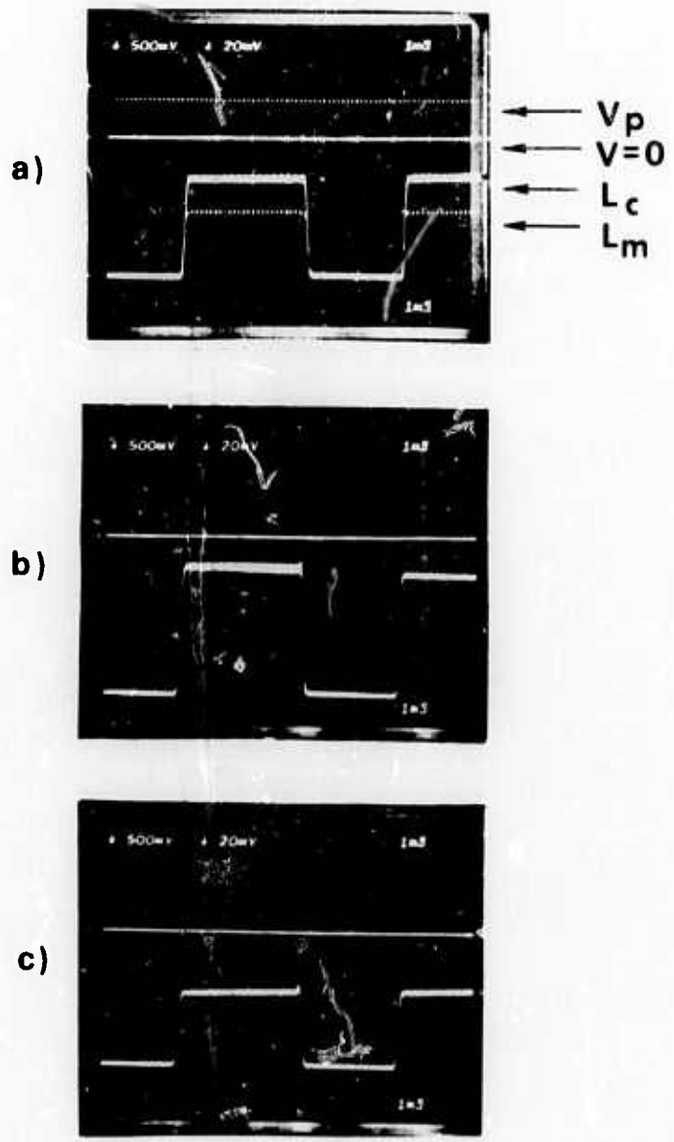

FIG. 9

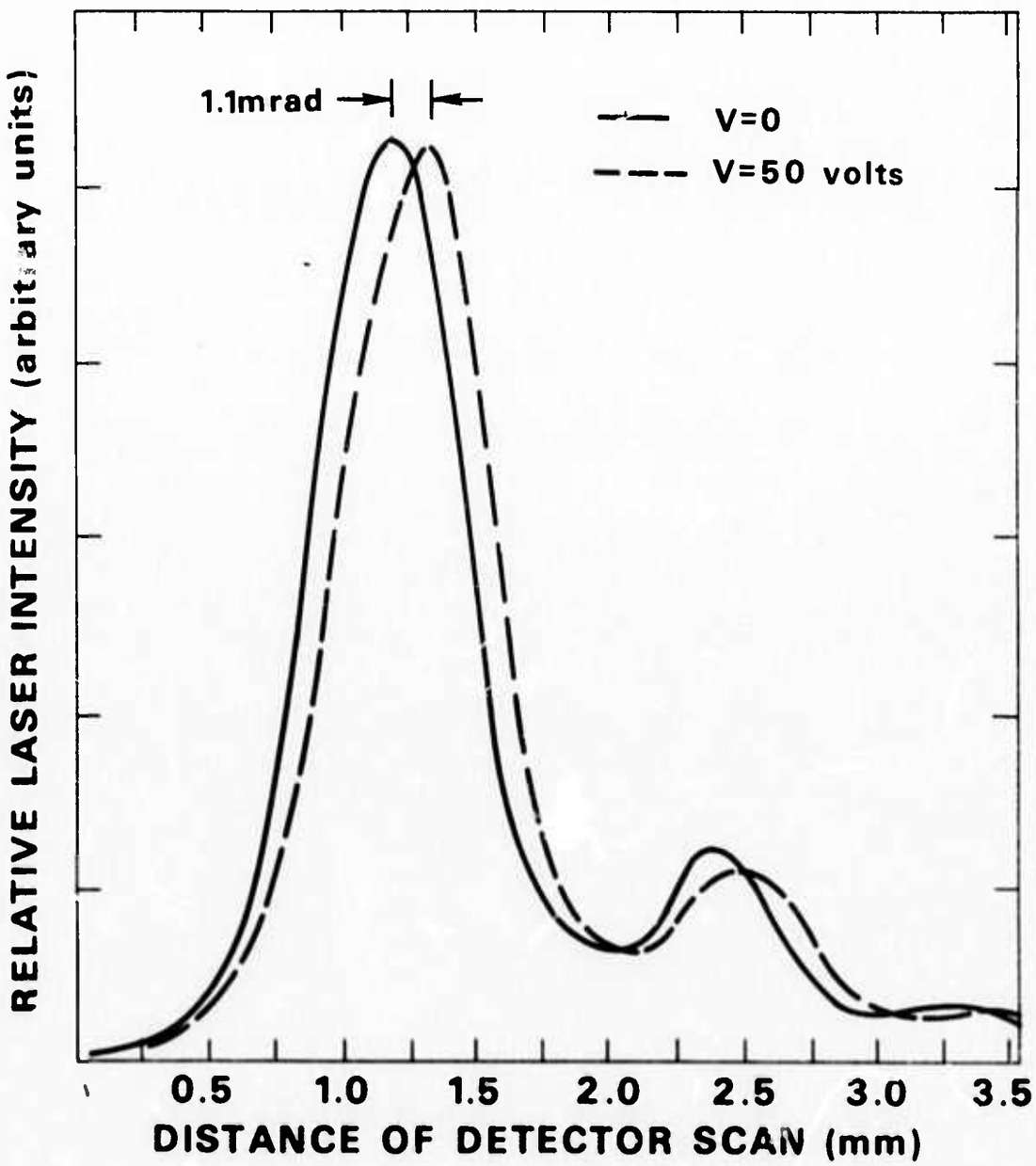
1.1mrad
V=0
V=50 volts
RELATIVE LASER INTENSITY (arbitrary units)
0.5
1.0
1.5
2.0
2.5
3.0
3.5
DISTANCE OF DETECTOR SCAN (mm)

$$\alpha \simeq \frac{\ell}{\omega_o}\Delta n_{EO} \qquad (10)$$

where ω_o is the beam width of the guide mode. For V = 50 volts, ℓ = 0.5 cm, t = 20 μm and ω_o = 0.3 mm, Eq. (10) gives a deflection angle $\alpha \simeq$ 1 mrad, which is in a good agreement with our measurements. To measure the depth of modulation, we first collect nearly all the transmitted power P_t with the help of a f/1 germanium lens by matching the detector aperture with the radiation coupled out of the output grating. When voltage is applied, a decrease in the detector output which coresponds to a maximum modulated signal P_m is obtained. The measured P_m/P_t ratio is about 12.8 percent at V_p = 50 volts. By choosing ℓ = 1 cm and t = 10 μm, we estimate that a 50% depth of modulation can be achieved by applying 50 volts to this thin film modulator.

2.2.2. Intensity Switching Experiments

Attempts were also made to study the device characteristics of a thin film electrooptic switch as suggested by A. Yariv (Ref. 9) for the 10.6 μm CO_2 laser radiation. The design of such a switch is based on the cutoff property of an optical waveguide. If the index profile of the waveguide device or the index difference Δn between the thin film and the supporting substrate is properly chosen to have a value in the proximity of the waveguide cutoff Δn_c, a small voltage applied to the device can induce a significant amount of electrooptic birefringence in the thin film that may be sufficient to switch a guided mode above and below its waveguide cutoff. The calculated Δn_c value is plotted in Fig. 10 as a function of the thin film thickness, t. Results indicate that Δn_c values depend critically on t. Three GaAs epitaxial thin films of properly controlled thickness, namely 18 μm, 22 μm and 34 μm have been used for this study. Each sample has been profiled by the Schottky barrier measurements described in previous sections and phase gratings have been etched into the epi-layers. The structure of these weak waveguides consists of an undoped ($N_f < 10^{12}$ cm^{-3}) epi-layer, grown on a low N(2.0-2.2 x 10^{16} cm^{-3}) substrate. The index difference between the film and the substrate as calculated from Eq. (1) is about 5 x 10^{-3}. The cutoff value Δn_c, for the TE_o mode can be calculated from the expression (Ref. 9)

$$\Delta n_c = \frac{1}{32n}\left(\frac{\lambda}{t}\right)^2 \qquad (11)$$

and is found to be 2.2 x 10^{-3}.

Figure 11 shows the transmission characteristics of two samples having thickness 22 μm and 34 μm. These transmission data have been normalized with respect to the value of a typical strong guide having a large refractive index (Δn ≃ 0.3) between the guiding layer and the substrate. Results show that transmission through these weak guides (Δn ≃ 10^{-3}) near cutoff is extremely poor and decreases rapidly as the thickness of the guide approaching the cutoff value t_c.

WAVEGUIDE CUT-OFF CHARACTERISTICS

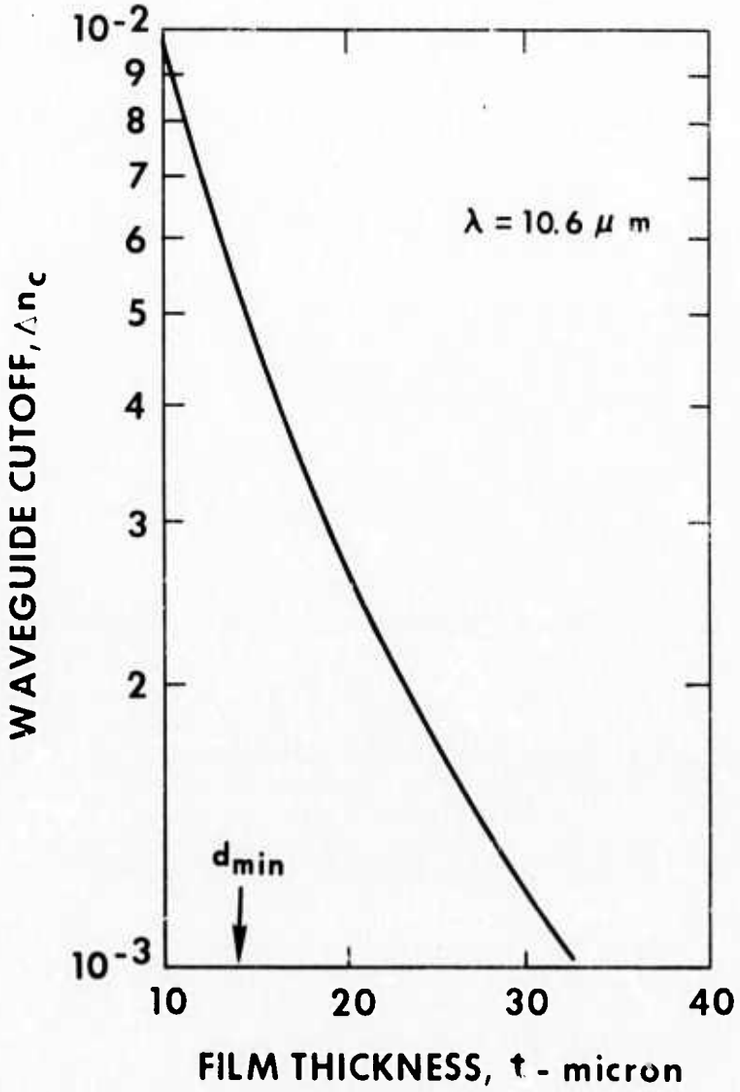

FIG. 11

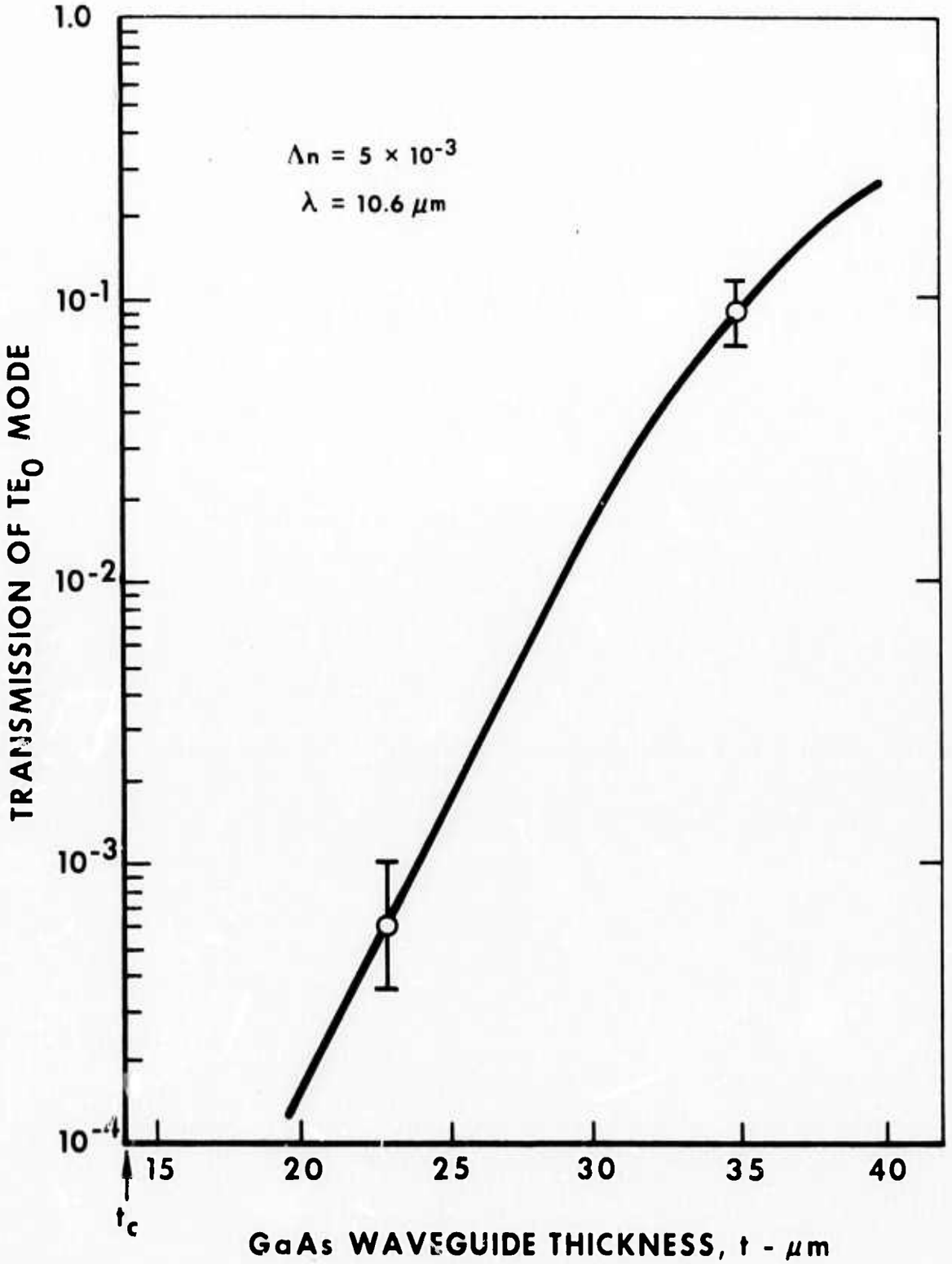
1.0
$\Delta n = 5 \times 10^{-3}$
$\lambda = 10.6\ \mu m$
10^{-1}
10^{-2}
10^{-3}
10^{-4}
TRANSMISSION OF TE_0 MODE
15
20
25
30
35
40
t_c
GaAs WAVEGUIDE THICKNESS, t - μm

For the 22 μm guide, the electrooptic change in index Δn_{EO} is 2.1×10^{-5} at V = 20 volts. Therefore the depth of modulation,

$$m = \frac{\Delta n_{EO}}{\Delta n - \Delta n_c} \tag{12}$$

at 20 volts is about 0.7 percent. To increase the depth of modulation, the thickness of the guide must be further reduced to below 20 μm. From the transmission data, however, it is doubtful that a guided mode can be established in such a weak guide having a thickness so close to the cutoff $t_c \simeq 15$ μm. Therefore we conclude that the scheme utilizing the waveguide cutoff is not very useful to obtain intensity modulation of light. At a first glance, it appeared rather attractive, but what one did not realize is that by operating the waveguide near its cutoff, optical transmission decreases significantly and is affected critically by film imperfections. For intensity modulation of CO_2 laser, beam steering technique as described above proved to be the best scheme than either the polarization modulation or switching near the waveguide cutoff. The advantage of thin film waveguide device utilizing the beam steering of a 10.6 μm guided-wave mode in thin film over the conventional bulk modulators is obvious. More can be gained by using such a device to modulate lasers at shorter wavelength. The improvement factor is expected to be proportional to $1/\lambda^2$. At shorter wavelengths, one not only gains a better resolution but also a higher field strength by using a thinner waveguide. The present modulation scheme is much more simple and convenient than the conventional phase modulation via thin films (Ref. 10), where a heterodyne receiver or an optical compensator is required. Experimental investigation of phase modulation of 10.6 μm CO_2 laser radiation in GaAs thin film will be described in the following section.

2.2.3 Phase Modulation

Presently we are in the process of performing an experiment to investigate phase modulation of the 10.6 μm CO_2 laser radiation in a GaAs thin film. This is an important experiment which should provide useful information directly related to our future plan for the generation of a sideband at the sum or the difference frequencies between an optical guided wave and either a traveling or a synchronous standing microwave.

The phase change $\Delta\Gamma$ is given by Eq. (3). Taking t = 20 μm, ℓ = 3 cm, a phase shift of π radian can be obtained with an applied voltage of 120 volts. The power converted into the sideband can be approximated by

$$\begin{aligned} E = E_o[J_o(\Delta\Gamma)\sin(\omega_o t+\Gamma_o)] \\ + J_1(\Delta\Gamma)\cos[(\omega_o+\omega_\mu)t+\Gamma_o] \\ + J_1(\Delta\Gamma)\cos[\omega_o-\omega_\mu)t+\Gamma_o] \\ + \cdots\cdots\cdots \end{aligned} \tag{13}$$

where ω_o, ω_μ are angular frequencies of the optical and microwave signals and for $\Delta\Gamma < 1$,

$$J_1(\Delta\Gamma) \simeq \frac{\Delta\Gamma}{2} - \frac{\Delta\Gamma^3}{2^2 2!} + O(\Delta\Gamma) \qquad (14)$$

From Eqs. (13) and (14) we estimate that approximately 5 percent of the optical power will be converted into the sideband. Assuming that a total 3 dB transmission loss through the waveguide, one watt CO_2 laser will give 50 mW microwave modulated output signal. In the following we shall discuss in detail an experiment designed to measure $\Delta\Gamma$.

The most accurate way to measure the phase shift in our laboratories is to use a super-heterodyne technique. This technique involves the measurement of the phase shift of the optical radiation at rf frequency. Figure 12 is a block diagram of the experimental setup. A CO_2 is incident into a Ge Bragg deflection cell. A fraction of its power will be deflected with a up-shifted frequency by the amount equal to the frequency f_a of the acoustic transducer. The undeflected beam is coupled into the GaAs thin film modulator. Upon application of a voltage V, the phase of the radiation coupled out off the thin film modulator is then shifted by $\Delta\Gamma$. After a mixing of the two beams in a HgCdTe detector (or CuGe), the output of the mixer contains a phase-shift signal at the rf frequency f_a. The amount of phase shift can be directly measured by using a vector voltmeter. Figure 13 shows the Ge Bragg cell which has recently been fabricated and tested. A $LiNbO_3$ transducer, which is bonded onto the surface of Ge Bragg cell, provides a frequency up-shifted CO_2 laser beam at $f_a \simeq 23$ MHz. Driving at one watt peak acoustic power, this cell provides a deflected beam at a power level about 2% of the incident power. At this power level this signal is more than sufficient to be used as a local oscillator for the heterodyne receiver. Figure 14 shows a GaAs thin film modulator (1-51-2A) specially prepared for this experiment. This modulator has a thickness ~ 17 μm and a 2 cm long Schottky barrier electrode. Results of this experiment will be reported in the final report.

FIG. 12

PHASE SHIFT MEASUREMENTS OF CO_2 LASER THROUGH AN ELECTROOPTIC GaAs THIN FILM MODULATOR

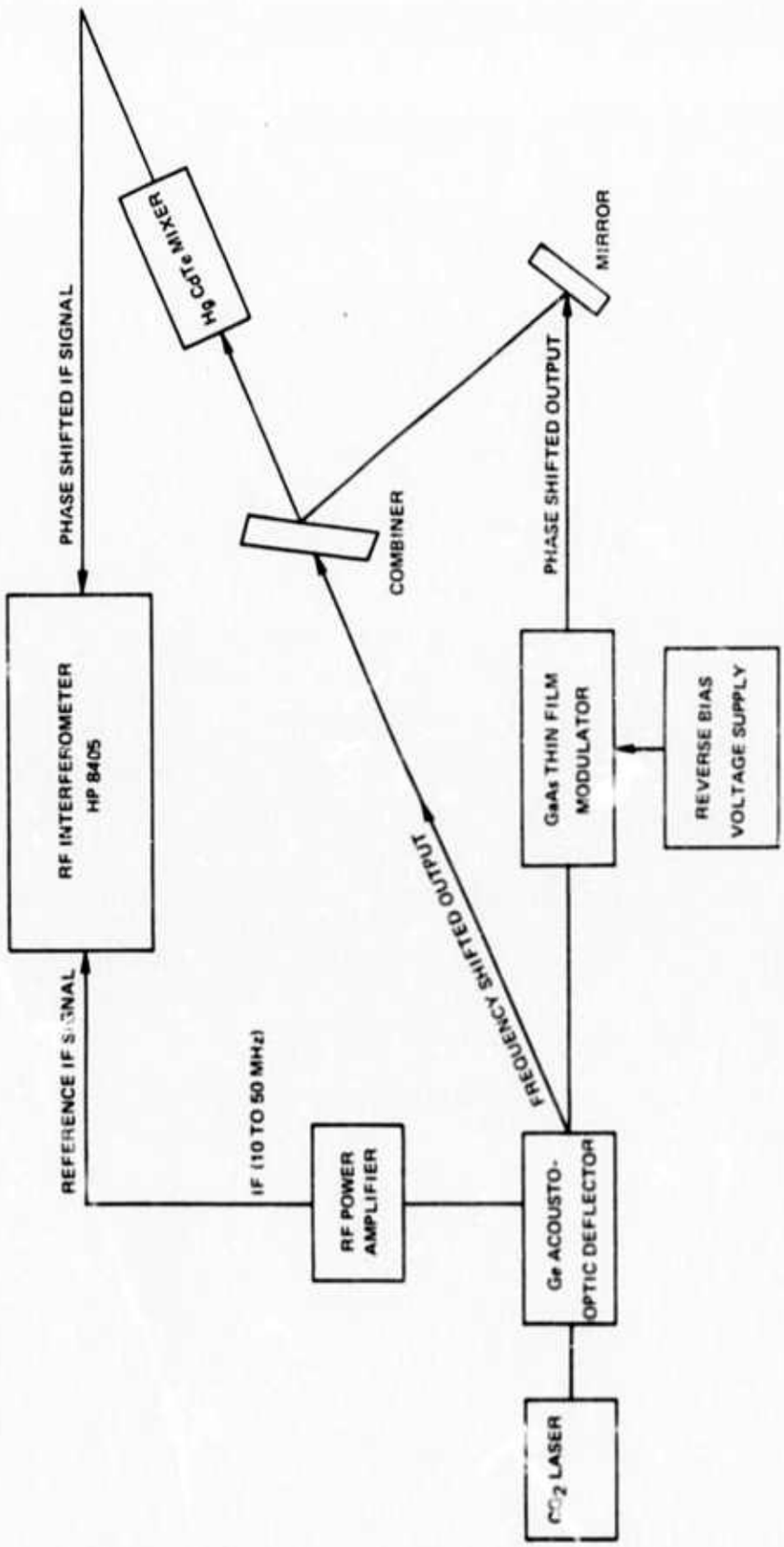

FIG. 13

Ge BRAGG DETECTOR

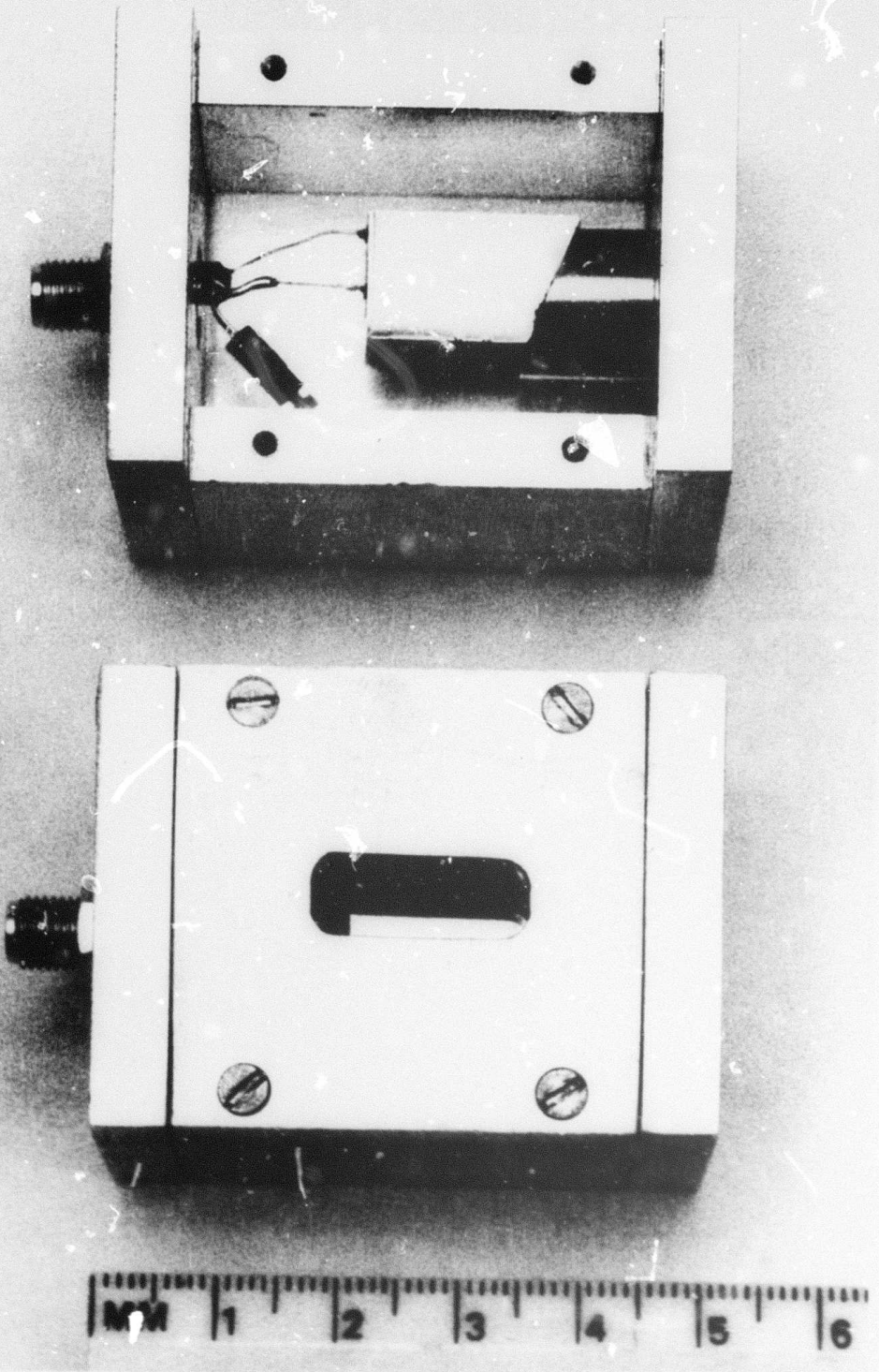

RL–73–71

FIG. 14

GaAs THIN MODULATOR

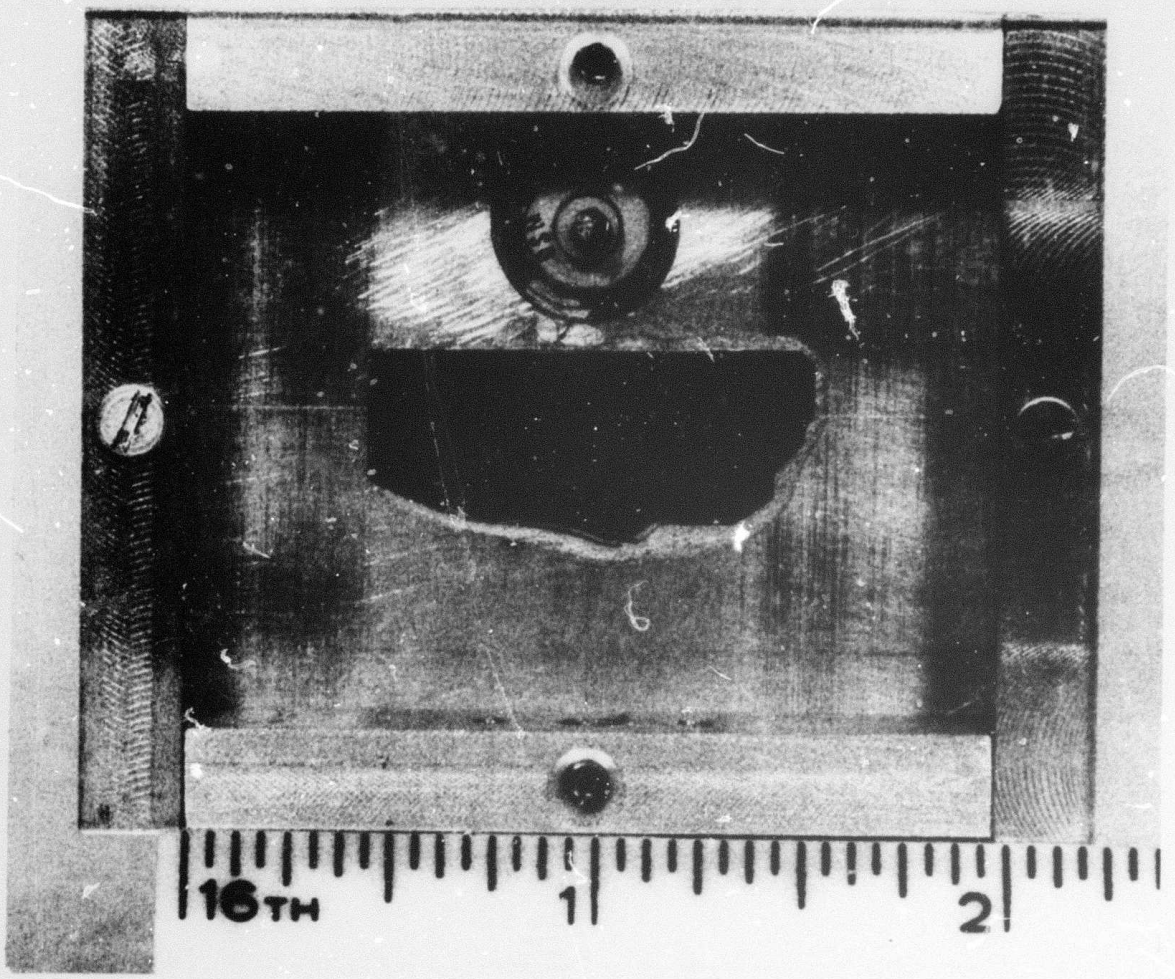

RL 73–93

3.0 OPTICAL AND MICROWAVE COUPLING TECHNIQUES

3.1 Optical Coupling

3.1.1 Introduction

Efficient optical coupling into and out of a thin film waveguide plays an important role in integrated optics. If waveguide devices are going to replace the bulk, techniques for obtaining efficient optical coupling must be developed. For the 10 μm CO_2 laser radiation, materials used for coupling of evanescent waves are very limited. Ge prisms can provide relatively efficient coupling (~ 50%), however, it is more difficult and inconvenient to use. The difficulty is primarily owing to the fact that cleavage of a single crystal GaAs thin film is very easy to occur under pressure. Phase grating couplers (Ref. 10) on the other hand have been widely used for the visible laser radiation and couplers of this type are more conforming to the integrated optics concepts. But the lack of photoresist materials suitable for IR radiation limits the use of grating couplers to only the etched groove type. Theoretical analysis of etched groove grating has been worked out by Chang (Ref. 11). Techniques of fabrication etched gratings have been developed at UARL and couplers of this type have been routinely used in our IR thin film work.

3.1.2 Forward Coupling

Presently the optical coupling efficiency of etched grating in a GaAs thin film for 10-μm laser radiation is in the range from 10 to 20% for a laser beam size varied from 1 to 5 mm in diameter. Optical coupling is achieved by phase-matching an incident laser beam from the air with a guided-wave mode in the GaAs thin film. The synchronous condition for the first order diffraction is

$$\beta_m = k\sin\theta + \frac{2\pi}{L} \qquad (m = 0,1,2,\ldots) \qquad (15)$$

where L is the periodicity of the grating, k and β_m are propagating constants in air and in thin film, respectively. For a 20 μm guide, β/k values for m = 0, 1, and 2 are 3.267, 3.194 and 3.125, respectively. Equation (15) indicates that for these β/k values, the values for L lie in the range from 3 to 4 μm. Etched gratings with a periodicity > 3 μm can easily be fabricated in GaAs thin film materials by photolithographic processes without relying on more sophisticated ion-beam or holographic techniques (Ref. 12). Theory (Ref. 11) indicates that the coupling efficiency depends critically on the mode order and also on the incident laser beam size. Figure 15 shows the calculated optimum coupling length as a function of the waveguide thickness for various TE modes. These results indicate that for optimum coupling efficiency, a coupling length (or beam size) greater than 3.5 mm is required for the TE_1 mode in a 20 μm thick waveguide. A coupling length greater than 6 mm (not shown in this figure) is required for the TE_o mode.

FIG. 15

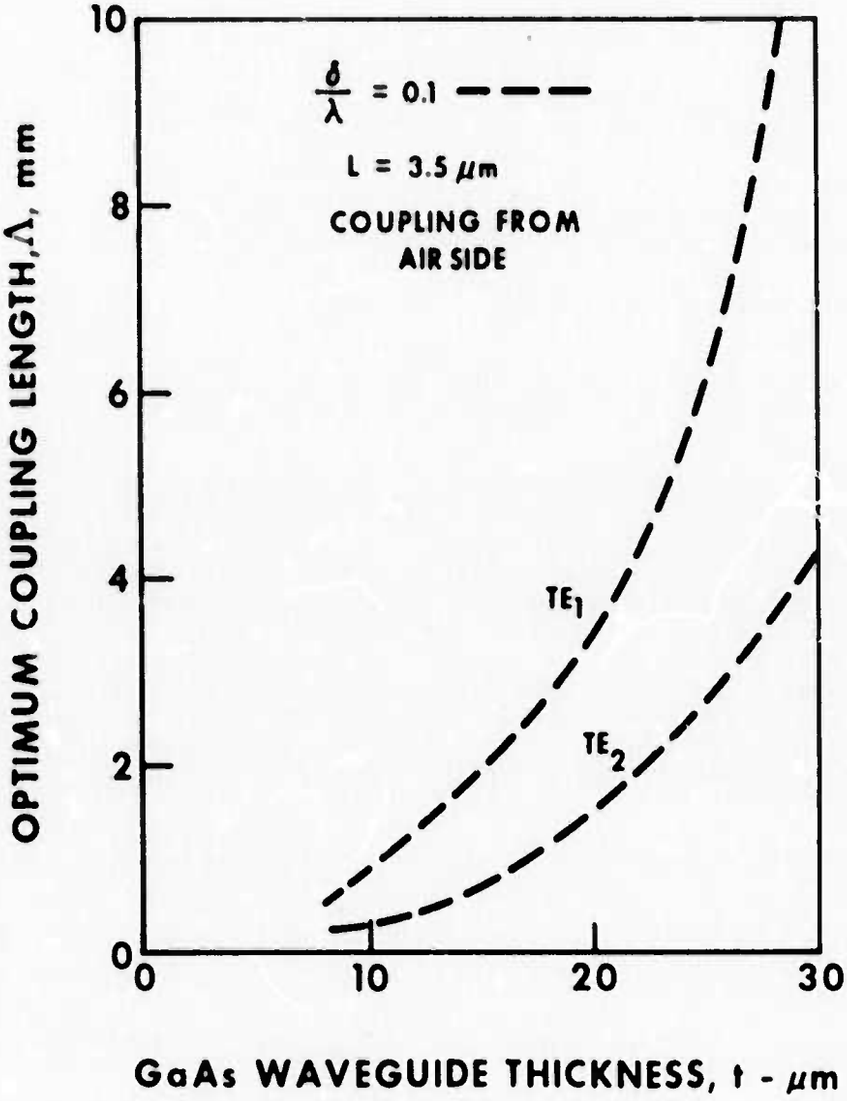
10
8
6
4
2
0
0
10
20
30
$\frac{\delta}{\lambda}$ = 0.1
L = 3.5 μm
COUPLING FROM
AIR SIDE
TE1
TE2
OPTIMUM COUPLING LENGTH, Λ, mm
GaAs WAVEGUIDE THICKNESS, t - μm

For all practical purposes, the laser beam size must be kept less than 1 mm so that the area of the Schottky barrier electrode would not be too excessive. As the electrode area increases the capacitance increases and the impedance decreases. For wideband modulation, it is difficult to design a rf network to match into a low ($\sim 2\Omega$) impedance load. For a coupling length 1 mm, coupling efficiency in the proximity of 10% has been achieved and our measurements are in a reasonable agreement with the theory. From the air side, the optimum coupling efficiency for the TE_o mode excited in the forward direction is 27% provided that a optimum coupling length $\gtrsim$ 1 cm is used. Obviously such a large coupling length is not suitable for the design of a wideband thin film modulator.

3.1.3 Backward Coupling

One way to reduce the optimum coupling length is to some extent, to decrease the grating periodicity. However, the choice of coupling length is constrained by the phase-matching condition, e.g., Eq. (15). If excitation is accomplished in the backward direction, as shown in Fig. 16, one can further reduce the value of L, because in these cases the phase-matching conditions are:

$$\beta_m = n_o \sin\theta + \frac{2\pi}{L} \qquad \text{(from substrate)} \qquad (16)$$

and

$$\beta_m = n_1 \sin\theta + \frac{2\pi}{L} \qquad \text{(from air)} \qquad (17)$$

Above discussion may be better understood by examining the allowed ranges of β values.

It was shown by Tien (Ref. 13) that there exists a number of modes for a given optical waveguide. One is a finite set of discrete modes known as guided modes having propagation constants β_m where m = 0, 1, 2, . . . The other is an infinite set of continuous modes consisting of the so-called "air modes" and "substrate modes". In the case of air mode ($0 \leq \beta \leq k$), the field is propagating in both the air and the substrate region. When $k \leq \beta \leq n_o k$, the field is evanescent in the air region and is propagating in the substrate. Figure 17 shows the region where these modes occur and the range of β values allowed by two excitation schemes. Among a number of other possibilities, Fig. 17(b) shows the worse case whereas Fig. 17(c) shows the most efficient excitation scheme. By choosing very small L values physically it means that (1) the guided-wave mode must be excited in the backward direction, (2) the power diffracted to various orders as well as to modes other than the guided-waves can be eliminated, and (3) the number of grooves is increased for a given beam size. In the case of GaAs thin film waveguide, L must be smaller than 3 μm. This raises the specification of the required photomask for photolithography one step beyond the state of the art.

FIG. 16

a) ETCHED GRATING IN THIN FILM

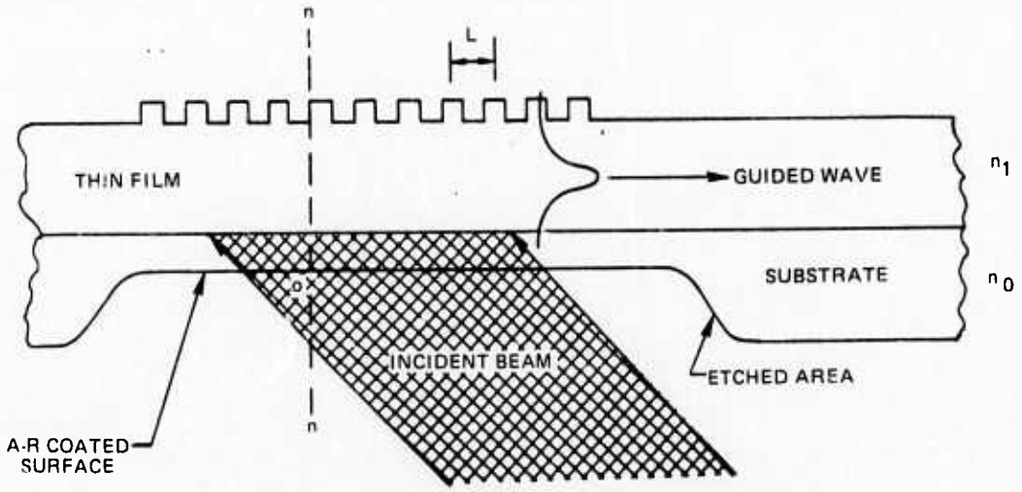

b) ETCHED GRATING IN SUBSTRATE

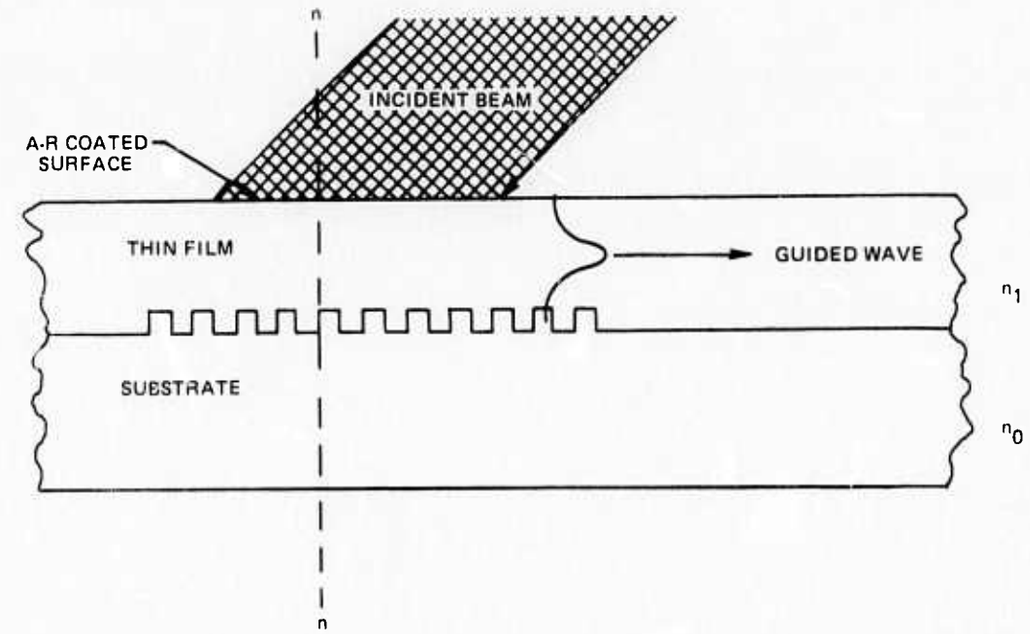

a) VARIOUS MODES OF UNPERTURBED THIN FILM WAVEGUIDE

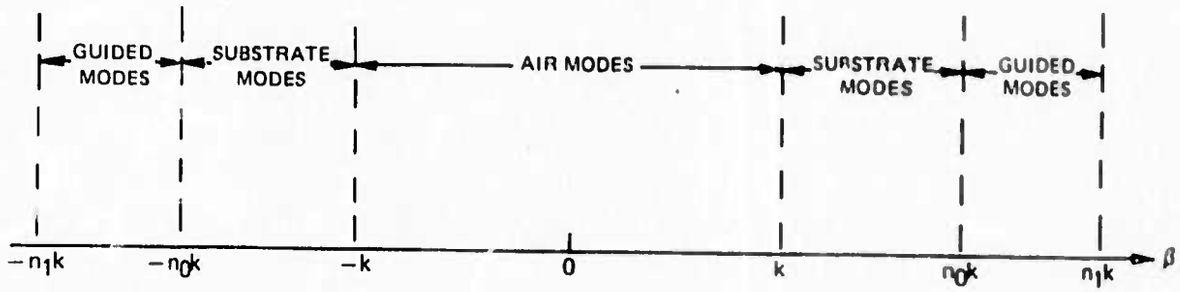

b) POSSIBLE MODES TO BE EXCITED FROM THE AIR SIDE IN THE FORWARD DIRECTION

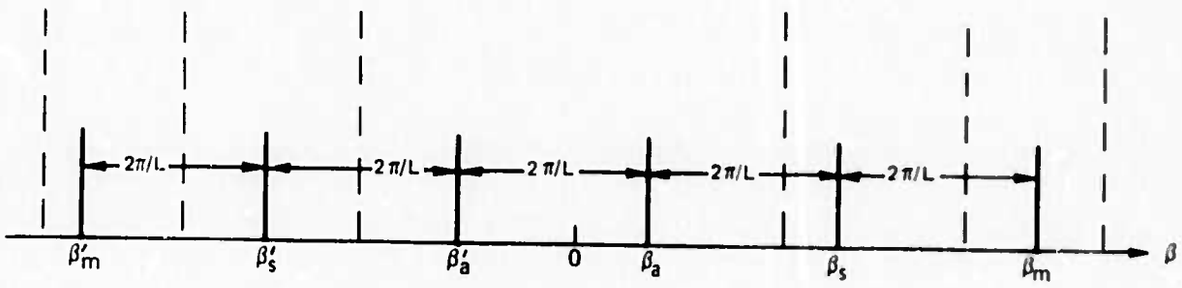

c) POSSIBLE MODES TO BE EXCITED FROM THE SUBSTRATE SIDE IN THE BACKWARD DIRECTION

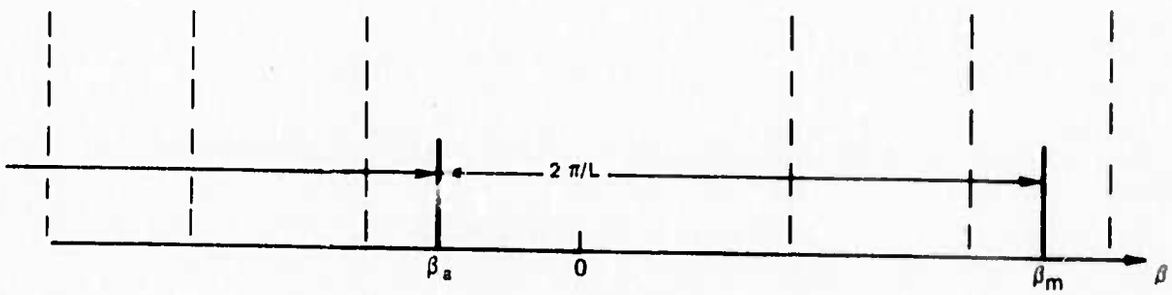

Large aperture (> 2 in) etched gratings on semiconducting surfaces with uniform spacing ranging from 0.5 to 2μ has been produced by Cheo and Bass (Ref. 12). These gratings were formed by a hologram exposure of photoresist film deposited on the semiconducting surface. The hologram was produced by adjusting the angle between two interferring He-Cd laser beams. The choice of the He-Cd laser (4416Å) over other lasers such as Ar^+ laser (4880Å) is to gain both the sensitivity at a lower wavelength and a longer coherent length.

Our laboratory is now equipped with a Cd-He laser which provides a single mode output over 100 mW at 4416Å. Associated optical components such as beam expander, beam splitter and spatial filter are on hand to produce the desired hologram gratings on the photoresist film (Shipley AZ1350). The photoresist film can be spin-coated on the GaAs thin film surface or on the low-resistivity GaAs substrate. The usual sputter-etch technique will be used to fabricate the gratings. Figure 16(a) shows the excitation of a guided mode by means of backward coupling from the substrate side into a thin film whose surface is etched. To avoid excessive optical loss in the substrate due to free carrier absorption ($\alpha \sim 50$ cm^{-1} for $N \sim 10^{18}$ cm^{-1}), a window will be opened in the substrate immediately below the grating coupler by etching away most of the low resistivity material. Surface reflection loss will be essentially eliminated by means of anti-reflection dielectric coating. The estimated absorption in a 5 μm substrate layer is 3 percent. Uniform etching of a large volume of material can be achieved by using a plasma anodization technique, which enhances the usual sputter-etching rate significantly. It is possible to control this process for removing the substrate material to within a 5 μm distance from the active thin film.

Figure 16(b) shows an alternative approach. In this case, the grating will be formed on the substrate and it will then be covered with an epitaxial thin film layer. This case is equivalent to that as shown in Fig. 17(c). The high refractive index of the film eliminates the possible excitation of other spurious modes when incident beam angle is chosen to phase-match a desired guided mode of the thin film. The phase-matching condition in this case is given by Eq. (17). The calculated coupling efficiency is 81 percent for the excitation scheme as described above. Experimentally, we expect to obtain a 3 dB coupler by using either one of the two schemes as our goal.

Progress has been made in the growth of high resistivity GaAs thin film on a N^+ GaAs substrate with the etched grooves. Figure 18 shows some of the recent results. Figure 18(a) shows the interface between a high resistivity GaAs thin film and N^+ GaAs substrate and Fig. 18(b) shows the etched groove grating with a periodicity $L = 3.5$ μm separating the epi-layer and the substrate. It is encouraging to see that the presence of etched groove does not appear to interfere with the growth of good quality GaAs thin film. Work is still in progress to make 2.5 μm gratings on N^+ GaAs substrate by means of holographic technique. The growth of high resistive thin films on these substrates will then be attempted. These results and the optical coupling data will be included in the final report.

M921513-2

INTERFACE BETWEEN AN UNDOPED GaAs THIN FILM
AND AN n^+ GaAs SUBSTRATE (490x)

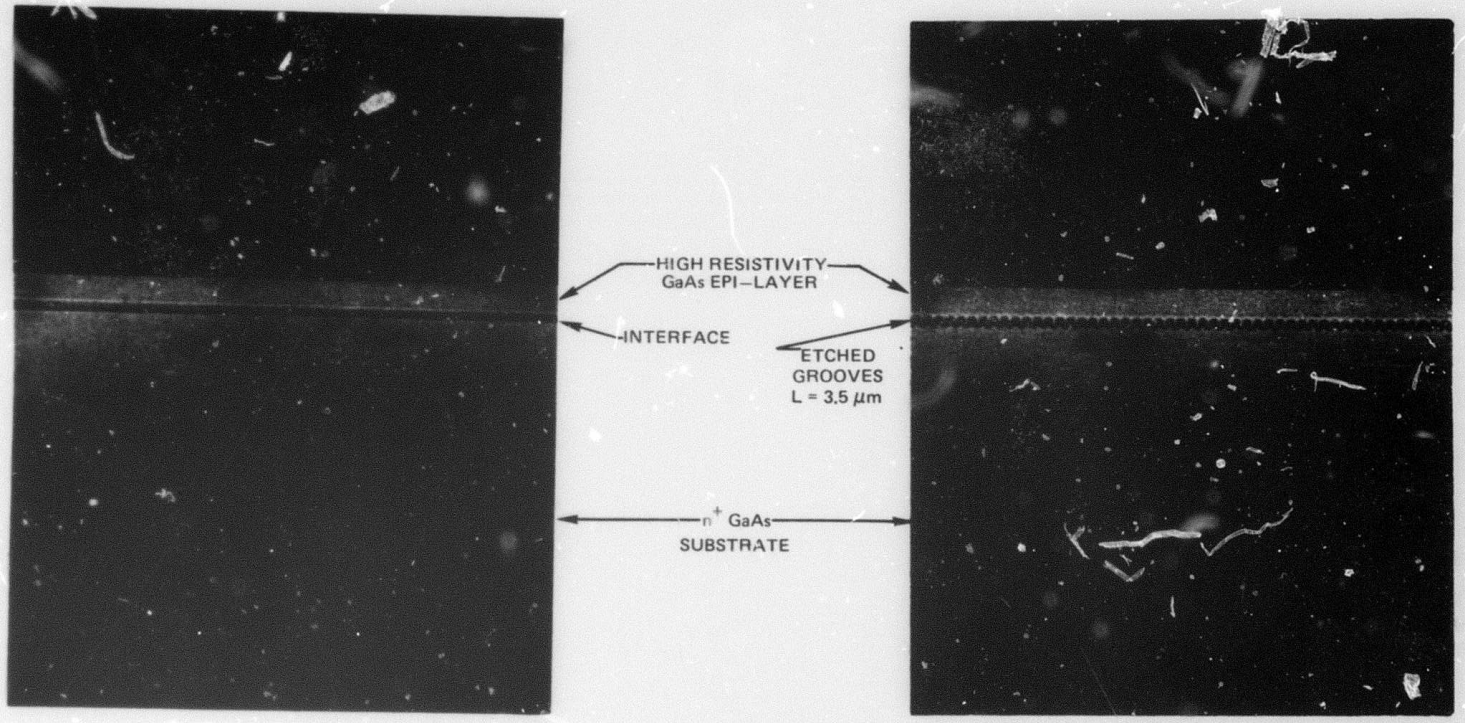

FIG. 18

3.2 Microwave Coupling Techniques

3.2.1 Introduction

An efficient modulating technique for generating 16.5 GHz sidebands on the IR carrier requires that the available microwave energy be concentration in the thin film electrooptic waveguide. However, the cross sectional dimensions of the electrooptical waveguide are very much smaller and different in aspect ratio than conventional microwave transmission lines. The implications of these facts and workable solutions will be discussed subsequently. First we will review the general interaction problem in terms of obtaining strong levels of sinusoidal phase modulation (π radians) with efficient use of microwave power.

The simplest type of electrooptic modulator is depicted schematically in Fig. 19(a). The accumulated phase shift is proportional to the electric field strength and the time spent by a differential section of the light beam in traversing the period of the modulating signal, then alternating positive and negative increments in modulation tend to cancel one another with little net modulation resulting. Therefore, the short transit time condition, indicated in Fig. 19(a) forces the use of undesirably high modulating fields and levels of microwave power. A high Q resonator could enhance the electric fields in a short transit-time modulator at the expense of useable bandwidth around the modulating frequency.

One technique for reducing the modulating field strength is to use an extended interaction region in which a synchronous condition exists between the light beam and a traveling wave modulating electric field (Ref. 14). This is depicted in Fig. 19(b), where the phase velocity of the traveling wave (microwave signal) is adjusted to be identical to the velocity of the light beam. Thus, each differential section of the light beam will continue to experience identical increments of modulation while traversing the entire modulator. More specifically the increments are determined by the phase at which the section of the beam enters the modulator. The interaction time can now be many times greater than the period of the modulating signal. One limitation on interaction time or transit-time, of course, would be the attenuation experienced by the microwave signal and another the attenuation experienced by the optical signal. (The attenuation of the light beam has been measured (Ref. 2) to be approximately 0.1 cm^{-1} for the TE modes in a thin film sandwiched between two metallic walls.)

The attenuation of the traveling wave microwave signal can be overcome in practical situations by using a transverse feed and generating a standing wave (or psuedo-standing wave where significant attenuation exists) along the modulator. This is depicted in Fig. 19(c) where the standing wave is setup by driving the long modulator at the points marked A, the position at which voltage maxima occur. Since the electrooptic modulation technique is linear, simple addition of the modulating effects due to the two components of the standing wave may be considered separately. The net modulation is then the arithmetic sum. The transverse line feed spacings can

FIG. 19

MODULATOR CONFIGURATIONS

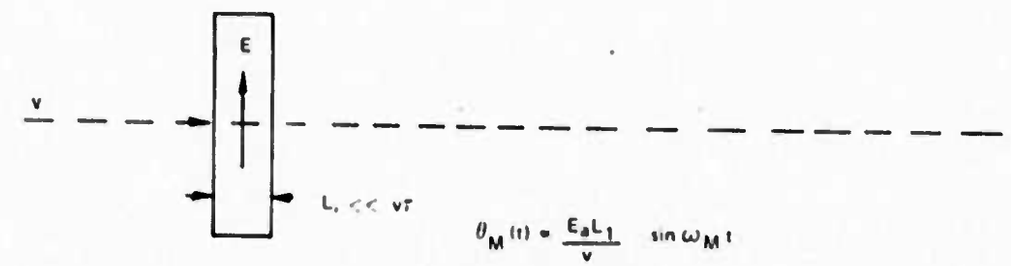

a) SHORT MODULATOR

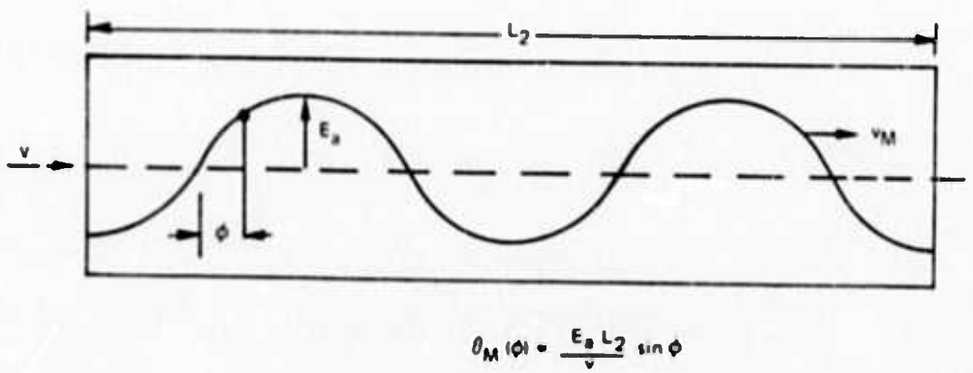

b) TRAVELING WAVE MODULATOR

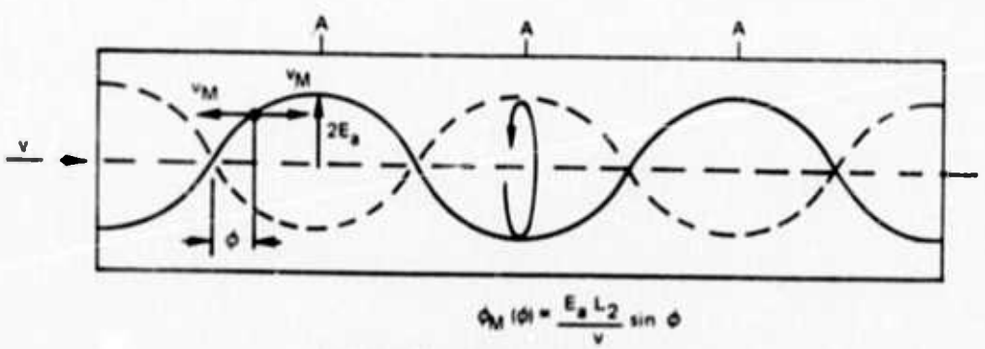

c) STANDING WAVE MODULATOR

be adjusted so that the forward component of the standing wave is synchronous with the light beam. The forward wave contributed modulation is discussed above. However, the backward wave, relative to the light beam, interacts periodically such that for each half of a microwave period the net modulation is zero. Thus, if the line length is a multiple of $\lambda/2$, the phase modulation incurred is as though only the forward traveling wave exists. Because of the nature of feeding the line transversely, some bandwidth narrowing exists.

The traveling wave interaction structure may be incorporated into microwave resonator utilizing a traveling wave resonator (or ring resonator). This is a well known technique for obtaining a higher power level in a traveling wave than is available from a particular microwave source. The traveling wave structure of Fig. 19(b) would be inserted into the ring resonator as shown in Fig. 20. A directional coupler is used to drive the ring resonator where the value of coupling must be set to an optimum value determined by the losses in the ring. The larger the losses the smaller the power gain is expected.

3.2.2 Synchronous Traveling Wave Structure

The phase velocity matching conditions are of prime importance in this work. Since the modulator is only 5 or 6 microwave wavelengths long some difference can be tolerated without series degradation of phase modulation. To correct for an anticipated difference of some 7% additional layers of low dielectric constant material will be used. If spurious effects requires a slower velocity, periodic loading of the line will be employed.

The dimensions of the thin-film optical waveguide lead to unusual parameters for the microwave waveguide. Because the dimensions are small, the active region is best treated as a narrow gap region of a microwave ridge-waveguide. The microwave waveguide is sketched in Fig. 21. The impedance of the waveguide is determined primarily by the parameters of the gap. Thus the characteristic impedance of the waveguide is calculated approximately from

$$Z_o \cong \frac{377}{\sqrt{\epsilon}} \frac{h}{W} \qquad (18)$$

to be 2.26 ohms (for W = 1000 μm, h = 20 μm, and $\sqrt{\epsilon} = 3.5$). The air filled gap, with the same dimensions, immediately in front of the modulator is 7.54 ohms. An intermediate $\lambda/4$ matching line may be included between these two sections by splitting the ridge into two narrower sections as shown in Fig. 21 by the section B-B. This construction, in fact, takes advantage of the metal that must be removed, in any case, from the optical grating region. The $\lambda/4$ section would be only 0.013 cm long for the GaAs. Several additional $\lambda/4$ matching sections are shown for raising the input and output impedance levels to values compatible with standard waveguide or coaxial transmission lines. These impedance matching transformers are designed by well known techniques (Ref. 15). Since they are of higher impedance values, these losses will be relatively insignificant.

FIG. 20

MICROWAVE TRAVELING WAVE RESONATOR

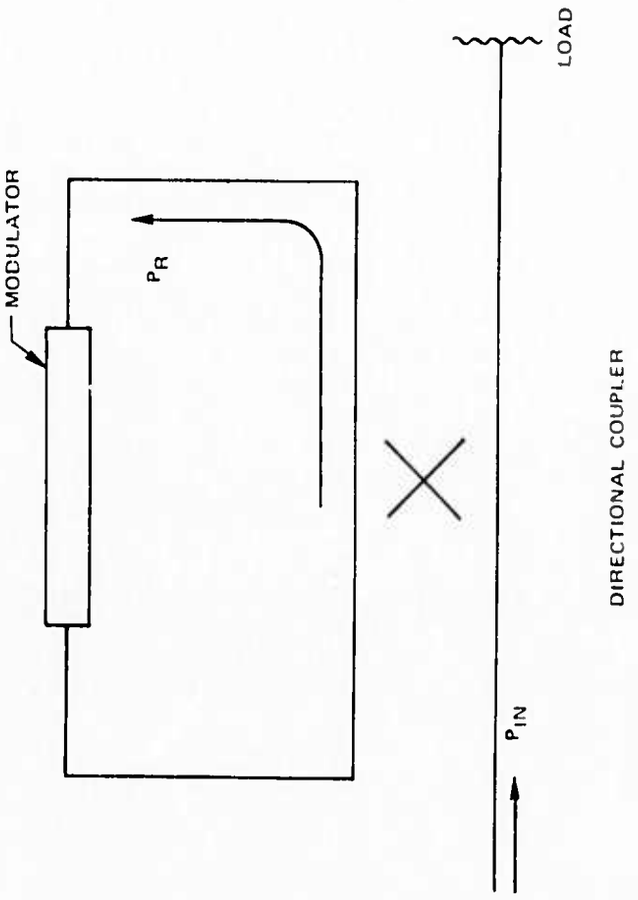

FIG. 21

TRAVELING WAVE MODULATOR CONFIGURATION

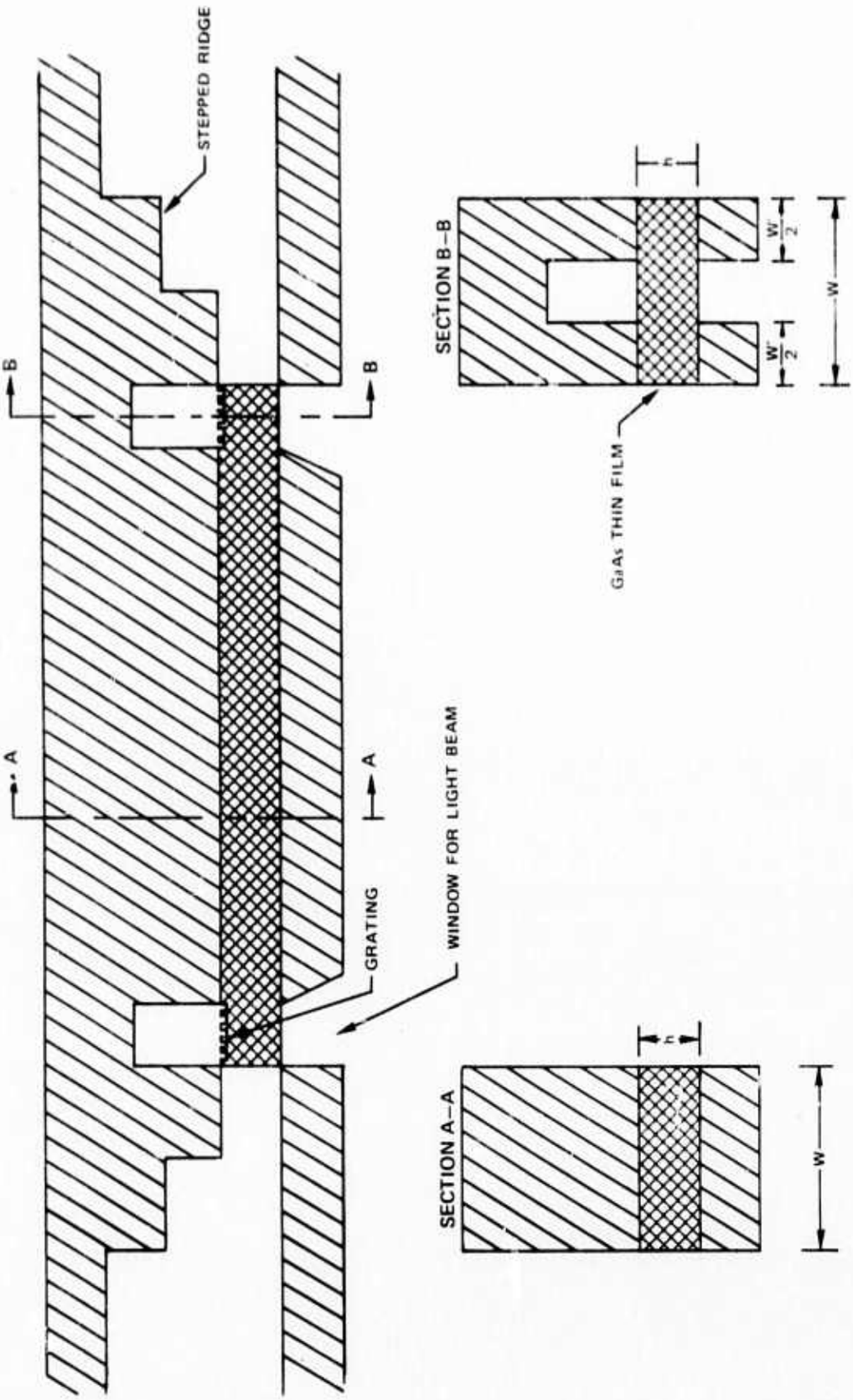

The small dimensions of the gap filled with GaAs, 20 μm, will require that a high degree of precision and surface finish be maintained in this structure in order to minimize transmission line losses. If the semi-insulated GaAs is backed directly with a metal such as copper the attenuation is calculated to be 1.42 dB per cm or .71 dB per wavelength. This level of attenuation is not prohibitive. One choice for fabricating the optical waveguide leaves a thin layer (2 to 5 μm) of n^+ GaAs substrate. This layer will increase the losses; however, since the skin depth in n^+ GaAs is 20 μm and the layer is backed by a metallic surface, these losses will not become excessive.

We will next examine the conditions required to provide the required total rf voltage swing of 20 volts peak to peak. This corresponds to an rms value of 7 volts. With a pure traveling wave in the 2.26 ohm GaAs filled ridged waveguide, neglecting attenuation, the power required is nominally 22 watts. Since the attenuation per centimeters is 1.42, the total attenuation for the desired 3 cm of length is 4.26 dB. This attenuation requires an increase of the input power to approximately 32 watts. The corresponding dissipated power is 20 watts. Fortunately this power is entirely dissipated at the metallic surfaces where heat removal is relatively direct and simple. The power dissipated in bulk of the GaAs is negligible.

The losses in the traveling wave structure are such that the use of a traveling wave resonator would not be effective in raising the ring power level significantly above that of the power directly available.

3.2.3 Synchronous Standing Wave Structure

We next turn to the transverse driven optical modulator. This is sketched in Fig. 22. The modulator is located at the end of a tapered wide ridge waveguide with its long axis perpendicular to the direction of propagation there. The single ridge is divided into 5 separate ridges that contact the modulator material at five positions spaced one wavelength apart. Each ridge section will carry approximately 1/5 the total power. The metallized modulator material itself forms a transmission line oriented perpendicular to the driving waveguide. In order to excite a standing wave in the modulator material the metallized portion ends in open circuits as shown in Fig. 22. The ridges contact the modulator at standing wave voltage maxima positions. Thus the five driving ridges reinforce a natural standing wave pattern along the modulator. If the power split between the ridges is uniform, because of symmetry, the one ridge may be studied as a typical element as shown in Fig. 23. The modulator section considered as the typical cell, consists of two open-circuited $\lambda/2$ sections of transmission lines in parallel.

The requirements for operating the synchronous standing wave configuration with the 2.26 ohm modulation line are calculated from Fig. 23. Each of the two $\lambda/2$ sections of open circuit line present a high impedance at the driving terminals. At the center frequency the value of each is 53 ohms of shunt resistance due to lines losses. Since only the forward wave is effective in modulation, the desired voltage of the

FIG. 22

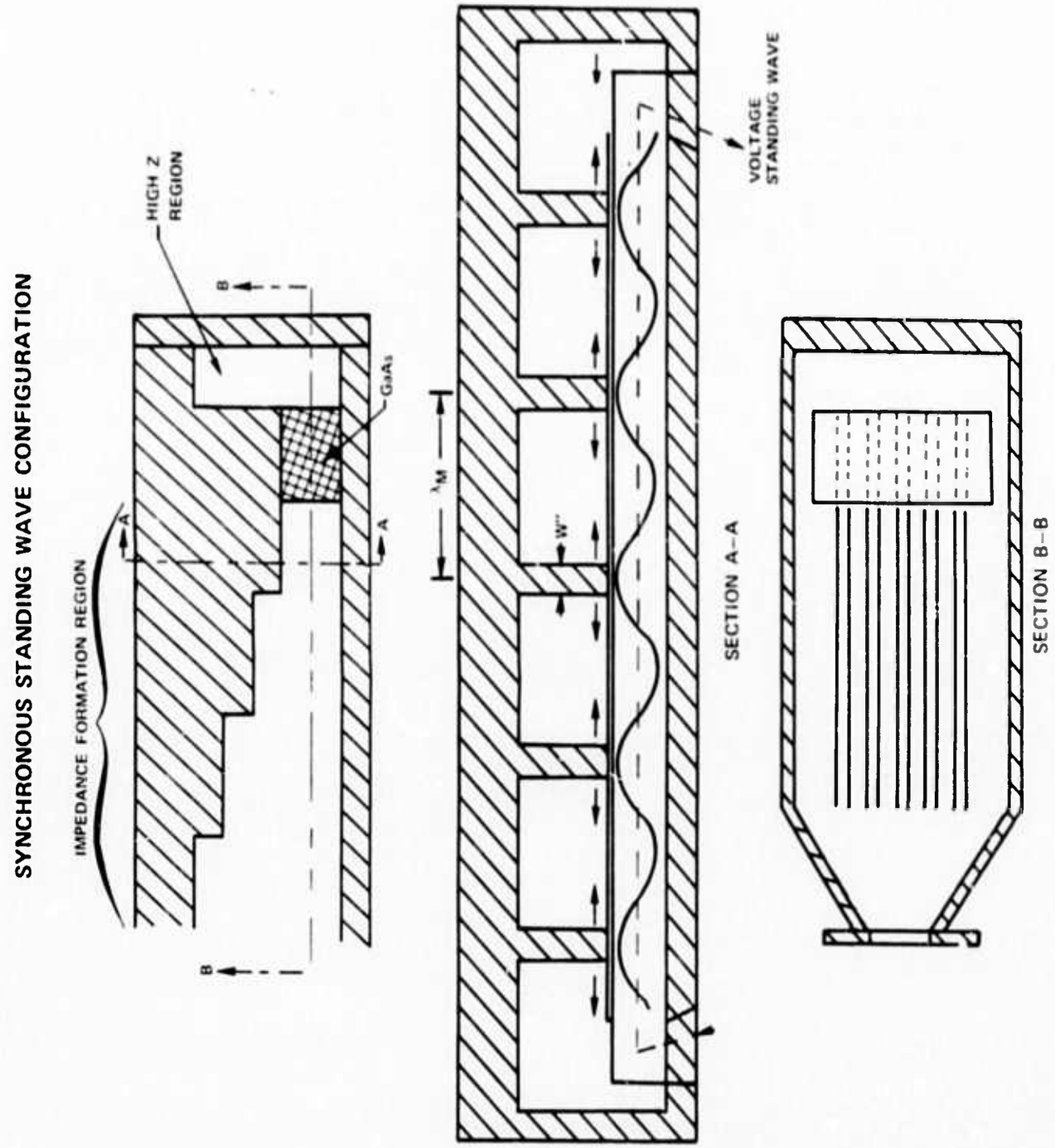
SYNCHRONOUS STANDING WAVE CONFIGURATION
IMPEDANCE FORMATION REGION
HIGH Z REGION
GaAs
A
A
B
B
λ_M
W
SECTION A-A
VOLTAGE STANDING WAVE
SECTION B-B

FIG. 23

TYPICAL CELL ANALYSIS OF TRANSVERSE FEED MODULATION CONFIGURATION

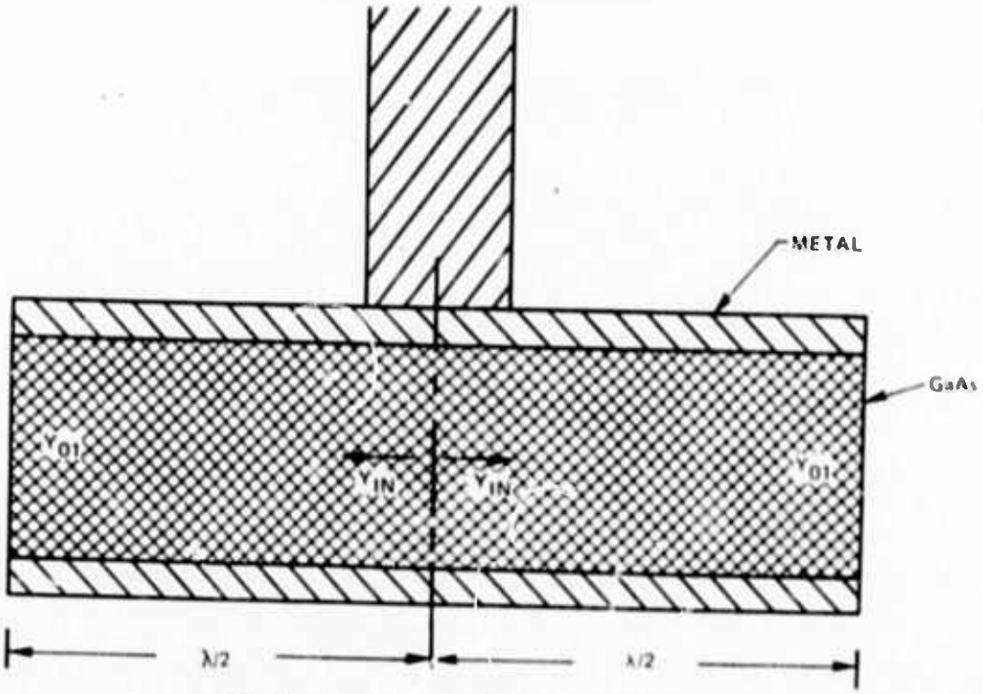

a) TYPICAL CELL OF RIDGE WAVE GUIDE

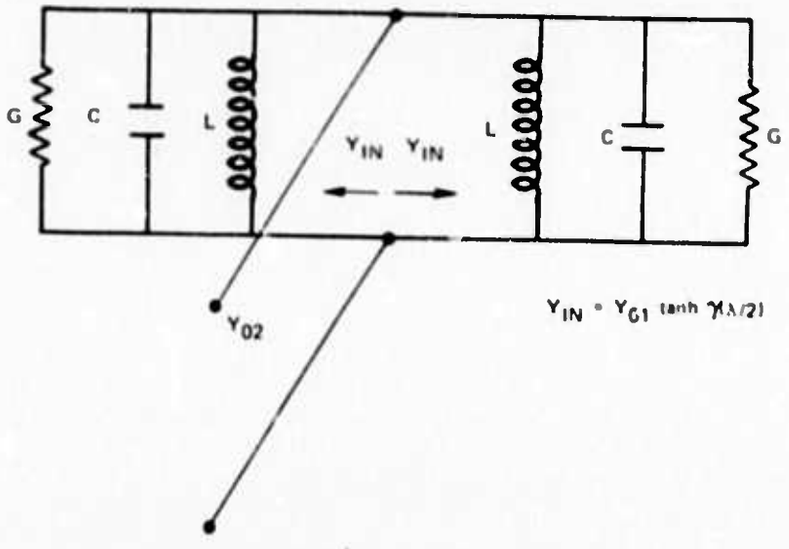

b) LUMPED EQUIVALENT CIRCUIT

forward wave is 7 volts rms as was discussed earlier. Thus the peak voltage at the driving point (Fig. 23) will be 14 volts and the power dissipation in a single section (two transmission lines) is 7.4 watts. For five sections the total dissipation is 37.0 watts. The impedance presented to each driving line is 26.5 ohms and the effective impedance of the five parallel sections is 5.3 ohms. The impedance levels in this configuration are more favorable then for the straight traveling wave structure discussed earlier.

The circuit configuration does result in additional storage of microwave energy with the result that the operating range of frequencies is reduced. The operating band may be calculated by estimating the Q of the circuit, again utilizing the equivalent circuits shown in Fig. 23. The stored energy in one transmission line is calculated approximately from (Ref. 16)

$$U = \frac{nP}{f} \tag{19}$$

where P is the nominal power in one component of the standing wave in the resonator and n is the number of half wavelengths (n = 1 for the circuit model in Fig. 23). The value for internal Q (no external load is used in this case) is calculated from

$$Q_i = \frac{WU}{P_d} = 2\pi \frac{P_i}{P_d} \tag{20}$$

to be 12. The value of loaded Q, which determined the operating 3 dB bandwidth, under matched conditions is 6 and the corresponding operating bandwidth is then 2.75 GHz.

Some preliminary work involving the design and fabrication of a microwave cavity is now in progress. The microwave structure for evaluating the electrical properties of the modulator is shown in Fig. 24. It is essentially a ridge waveguide with the modulator material placed in the narrow gap between the ridge and the ground plane. The purpose of these experiments is to determine an optimum structure for efficient coupling of microwave power into the GaAs sample. The dimensions of the gap in the ridge waveguide are the same as the optical waveguide. In these experiments the ridge section becomes an open circuit transmission line connected to a 50 ohm input line. Impedance measurements over a range of frequencies referenced to a plane established at the input to the ridge section will yield data on attenuation and effective wavelength. This information in turn will allow impedance transformers to be designed for the efficient coupling of power and will suggest possible modifications in the structure. A similar structure, with the sample removed, will be used to determine similar information on air filled ridge waveguides. The air filled sections will serve as the impedance transformers.

RIDGE WAVEGUIDE TEST SECTION

a) TEST SECTION

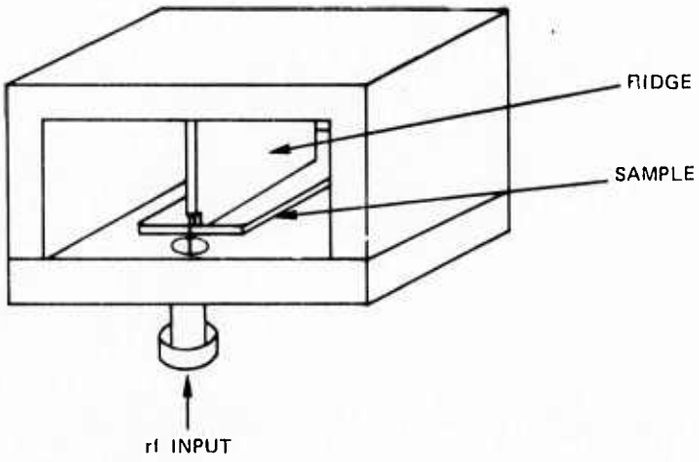

b) DETAILS OF RIDGE SECTION

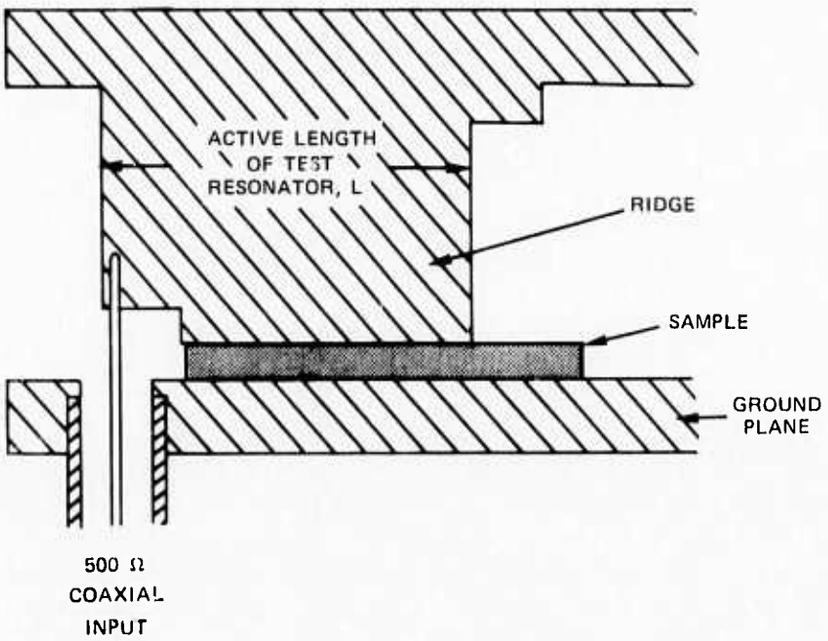

Preliminary calculations assuming 1 mil sample thickness have indicated that open circuited lines, because of losses, will already be fairly well matched to the 50 ohm input line. The major contribution to the losses, assuming semi-insulating semiconductors, will be copper losses in the ridge section. Therefore, the surfaces in the ridge section will be ground flat and be highly polished.

In conclusion, we have shown that less than 40 watts of microwave power can provide the desired level of modulation. For the synchronous traveling wave approach, the bandwidth is limited only by the large impedance transformation. Obtaining a 1.5 GHz bandwidth should present no problem. For the synchronous standing wave approach, the bandwidth of the modulator itself is 2.5 GHz; however, because some impedance transformation is required to a suitable input line, the effective value will be lower. Again the 1.5 GHz bandwidth should be attainable.

REFERENCES

1. P. K. Cheo, Appl. Phys. Letters 22, 241 (1973).

2. P. K. Cheo, J. M. Berak, W. Oshinsky and J. L. Swindal, Appl. Optics 12 500 (1973).

3. United Aircraft Research Laboratories, Proposal P-M49, March 1973.

4. J. A. Copeland, IEEE Trans. Electr. Dev. ED-16, 445 (1969).

5. J. A. Copeland, IEEE Trans. Electr. Dev. ED-17, 404 (1970).

6. N. Goldsmith and W. Oshinsky, RCA Rev. 24, 546 (1963).

7. M. Shah, J. D. Crow and S. Wang, Appl. Phys. Letters 20, 66 (1972).

8. L. Kuhn, P. F. Heidrich and E. G. Lean, Appl. Phys. Letters 19, 428 (1971).

9. D. Hall, A. Yariv and E. Garmire, Appl. Phys. Letters 17, 127 (1970).

10. M. Dakss, L. Kuhn, P. F. Heidrich and B. A. Scott, Appl. Phys. Letters 16, 523 (1970).

11. K. Ogawa, W. S. C. Chang, B. L. Sopori and F. J. Rosenbaum, IEEE J. Quant. Elect. QE-9, 29 (1973).

12. P. K. Cheo and C. D. Bass, Appl. Phys. Letters 18, 567 (1971).

13. P. K. Tien, Appl. Optics 10, 2395 (1971).

14. F. S. Chen, Proc. IEEE 58, 1440 (1970).

15. C. G. Montgomery, R. H. Dicke and E. M. Purcell, Principles of Microwave Circuits, McGraw-Hill (1948) p. 49.

16. G. B. Jacobs and H. C. Bowers, J. Appl. Phys. 38, 2692 (1967) ($^{13}C\ ^{16}O_2$).